20. Inaba M, Nishizawa Y, Mita K et al. (1999) Poor glycemic control impairs the response of biochemical parameters of bone formation and resorption to exogenous 1,25-dihydroxyvitamin D_3 in patients with type 2 diabetes. Osteoporos Int 9:525–531
21. Nagata-Sakurai M, Inaba M, Goto H et al. (2003) Importance of inflammation and bone resorption in an increase of arterial intima-media thickness (IMT) in patients with rheumatoid arthritis (RA). Arthr Rheum 48:3061–3067
22. Cheng S, Njeh CF, Fan B et al. (2002) Influence of region of interest and bone size on calcaneus BMD: implications for the accuracy of quantitative ultrasound assessments at the calcaneus. Br J Radiol 75:59–68
23. Tsuda-Futami E, Hans D, Njeh CF et al. (1999) An evaluation of a new gel-coupled ultrasound device for the quantitative assessment of bone. Br J Radiol 72:691–700
24. Nagasaki T, Inaba M, Henmi Y et al. (2003) Decrease in carotid intima-media thickness in hypothyroid patients after normalization of thyroid function. Clin Endocrinol 59:607–612
25. Kawagishi T, Nishizawa Y, Konishi T et al. (1995) High-resolution B-mode ultrasonography in evaluation of atherosclerosis in uremia. Kidney Int 48:820–826
26. Hirai T, Sasayama S, Kawasaki T et al. (1989) Stiffness of systemic arteries in patients with myocardial infarction: a noninvasive method to predict severity of atherosclerosis. Circulation 80:78–86
27. Hosoi M, Nishizawa Y, Kogawa K et al. (1996) Angiotensin-converting enzyme gene polymorphism is associated with carotid arterial wall thickness in non-insulin-dependent diabetes patients. Circulation 94:704–707
28. Poli A, Tremoli E, Colombo A et al. (1988) Ultrasonographic measurement of the common carotid artery wall thickness in hypercholesterolemic patients: a new model for the quantitation and follow-up of preclinical atherosclerosis in living human subjects. Atherosclerosis 70:253–261
29. Bland JM, Altman DG (1986) Statistical methods for assessing agreement between two methods of clinical measurement. Lancet 1:307–310
30. Friedlander AL, Genant HK, Sadowsky S et al. (1995) A two-year program of aerobics and weight training enhances bone mineral density of young women. J Bone Miner Res 10:574–585
31. Shigematsu T, Miyamoto A, Mukai C et al. (1997) Changes in bone and calcium metabolism with space flight. Osteoporos Int 7:S63–7
32. Boot AM, de Ridder MAJ, Pols HA et al. (1997) Bone mineral density in children and adolescents: relation to puberty, calcium intake, and physical activity. J Clin Endocrinol Metab 82:57–62
33. Damilakis J, Perisinakis K, Kontakis et al. (1999) Effect of lifetime occupational physical activity on indices of bone mineral status in healthy postmenopausal women. Calcif Tissue Int 64:112–116
34. Daly RM, Rich PA, Klein R (1997) Influence of high impact loading on ultrasound bone measurements in children: a cross-sectional study. Calcif Tissue Int 60:401–404
35. Lappe JM, Recker RR, Weidenbusch D (1998) Influence of activity level on patellar ultrasound transmission velocity in children. Osteoporos Int 8:39–46
36. Hoshino H, Kushida K, Yamazaki K et al. (1996) Effect of physical activity as a caddie on ultrasound measurements of the os calcis: a cross-sectional comparison. J Bone Miner Res 11:412–418
37. Okabe R, Inaba M, Sakai S et al. (2004) Enhanced atherosclerosis in paretic lower in the patients with hemiparesis. Clin Sci (Lond) 166:613–618
38. Laroche M, Pouilles JM, Ribot C et al. (1994) Comparison of the bone mineral content of the lower limbs in men with ischemic atherosclerotic disease. Clin Rheum 13:611–614
39. Laroche M, Barbier A, Ludot I et al. (1996) Effect of ovariectmy on intraosseous vascularization and bone remodelling in rats: action of tiludronate. Osteoporos Int 6:127–129
40. Reeve J, Arlot M, Wootton R et al. (1988) Skeletal blood flow, iliac histomorphometry and strontium kinetics in osteoporosis: a relationship between blood flow and corrected apposition rate. J Clin Endcrinol Metab 66:1124–1131
41. Burkhardt R, Barti R, Frisch B et al. (1984) The structural relationship of bone forming and endothelial cells of the bone marrow. In: Bone circulation. Williams and Wilkins, Baltimore, pp 2–14

The centrosomal protein Lats2 is a phosphorylation target of Aurora-A kinase

Shingo Toji[1,†], Norikazu Yabuta[2,†], Toshiya Hosomi[2], Souichi Nishihara[2], Toshiko Kobayashi[1], Susumu Suzuki[1], Katsuyuki Tamai[1] and Hiroshi Nojima[2,*]

[1]*Ina Laboratories, MBL Co. Ltd, Ina, Nagano 396-0002, Japan*

[2]*Department of Molecular Genetics, Research Institute for Microbial Diseases, Osaka University, 3-1 Yamadaoka, Suita City, Osaka 565-0871, Japan*

Human Lats2, a novel serine/threonine kinase, is a member of the Lats kinase family that includes the *Drosophila* tumour suppressor *lats/warts*. Lats1, a counterpart of Lats2, is phosphorylated in mitosis and localized to the mitotic apparatus. However, the regulation, function and intracellular distribution of Lats2 remain unclear. Here, we show that Lats2 is a novel phosphorylation target of Aurora-A kinase. We first showed that the phosphorylated residue of Lats2 is S83 *in vitro*. Antibody that recognizes this phosphorylated S83 indicated that the phosphorylation also occurs *in vivo*. We found that Lats2 transiently interacts with Aurora-A, and that Lats2 and Aurora-A co-localize at the centrosomes during the cell cycle. Furthermore, we showed that the inhibition of Aurora-A-induced phosphorylation of S83 on Lats2 partially perturbed its centrosomal localization. On the basis of these observations, we conclude that S83 of Lats2 is a phosphorylation target of Aurora-A and this phosphorylation plays a role of the centrosomal localization of Lats2.

Introduction

The onset and exit of mitosis are tightly regulated by the phosphorylation and dephosphorylation of numerous proteins. These mitotic phosphorylations are carried out by various mitotic serine/threonine kinases such as Cdk, Polo, NIMA and Aurora (reviewed in Nigg 2001). Members of these kinase families are highly conserved from yeast to human and participate in centrosome maturation and separation, spindle assembly, nuclear envelope breakdown, chromosome condensation and cytokinesis. According to recent studies in yeast and *Drosophila melanogaster*, mutations in these kinases can lead to phenotypes that are characteristic of defects in mitosis, including monopolar spindles, unequally separated bipolar spindles and failure in cytokinesis. This suggests that inaccurate controls of mitotic processes can lead to aneuploidy or genetic instability, finally causing tumour formation or apoptosis (Nigg 2001). Therefore, to understand oncogenesis and tumour progression, it is crucial to define the signalling pathways of these mitotic kinases.

The *Drosophila* Aurora gene, which is highly homologous to *Saccharomyces cerevisiae* IPL1, was identified in a search for the gene that regulates the formation of a functional centrosome and mitotic spindle (reviewed in Bischoff & Plowman 1999; Giet & Prigent 1999). Amorphic alleles of aurora result in pupal lethality and in mitotic arrest in which the condensed chromosomes are arranged on circular monopolar spindles. The loss of function of the Aurora kinase causes failures in centrosome separation and bipolar spindle formation (Glover *et al.* 1995). In mammals, the Aurora kinase family consists of at least three members, including Aurora-A, Aurora-B and Aurora-C (Adams *et al.* 2001; Nigg 2001). Aurora-A is prominent both at the centrosomes and in the nucleus of G_2 phase cells and at the half-spindle (a zone between the kinetochore and the spindle pole) in metaphase and telophase cells (Crosio *et al.* 2002; Hirota *et al.* 2003).

†The first two authors contributed equally to this work.

Communicated by: Eisuke Nishida

**Correspondence*: E-mail: hnjm2606@biken.osaka-u.ac.jp

DOI: 10.1111/j.1356-9597.2004.00732.x

Therefore, Aurora-A is considered to be involved in centrosome maturation and mitotic spindle assembly (Dutertre *et al.* 2002; Blagden & Glover 2003). Aurora-B is prominent in the nucleus during interphase, at the midzone during anaphase and in post-mitotic bridges during telophase, and is considered to be involved in chromosomal events and cytokinesis (Adams *et al.* 2001). Aurora-C is localized to the centrosome during the later stages of mitosis but its function is not yet clear (Kimura *et al.* 1999). Therefore, these Aurora kinase homologues are implicated in mitotic regulation including centrosome duplication, centrosome maturation, chromosome segregation and cytokinesis (reviewed in Dutertre *et al.* 2002; Blagden & Glover 2003).

Human Aurora-A is reported to be located on chromosome 20q13, a region that is frequently amplified in breast cancers and in diverse cancer cell lines. Over-expression of Aurora-A leads to abnomal centrosome amplification, chromosomal instability and transformation of NIH3T3 cells (Bischoff *et al.* 1998; Zhou *et al.* 1998). In $p53^{-/-}$ cells, over-expression of Aurora-A also causes extra centrosomes through defects in cytokinesis and consequent tetraploidization (Meraldi *et al.* 2002). This effect is blocked by p53, which directly binds and inhibits Aurora-A (Chen *et al.* 2002). Moreover, in primary cultures of mouse embryo fibroblasts, over-expression of Aurora-A inaccurately enters anaphase despite defective spindle formation, indicating that the elevated Aurora-A expression overrides the mitotic spindle assembly checkpoint (Anand *et al.* 2003). Recently, some attractive studies on the novel phosphorylation targets of human Aurora-A have been reported. One of the reports showed that human Aurora-A can phosphorylate PP1, a protein phosphatase type 1 and phosphorylations of PP1 by Aurora-A inhibit its phosphatase activity in HeLa cells (Katayama *et al.* 2001). Moreover, TPX2, a prominent component of the spindle apparatus, has been shown to be required for recruiting Aurora-A to spindle microtubeles in HeLa cells and to be the likely regulator of Aurora-A activity at mitotic spindle in *Xenopus* eggs, albeit the biological function of phosphorylation of TPX2 by Aurora-A remains unclear (Kufer *et al.* 2002; Eyers *et al.* 2003; Tsai *et al.* 2003). TACC3, a human homologue of the centrosomally associated protein D-TACC, has also been shown to be phosphorylated by Aurora-A (Giet *et al.* 2002). Phosphorylation of D-TACC by Aurora-A is probable because the recruitment of D-TACC to the centrosome requires the phosphorylation of additional centrosomal substrates (Blagden & Glover 2003). These observations suggest that Aurora-A protein is crucial for genomic stability and the maintenance of the cell cycle progression in mammalian cells.

Mammalian Lats2, a novel serine/threonine kinase, is a member of Lats kinase family to which the *Drosophila* tumour suppressor *lats/warts* also belongs (Yabuta *et al.* 2000). Mutation of the *lats* gene leads to dramatic over-proliferation of phenotypes and diverse developmental defects in *Drosophila* mosaic animals and homozygous mutants (Justice *et al.* 1995; Xu *et al.* 1995). Similar to the *Drosophila* mutants, mice deficient in *LATS1* gene, a counterpart of *LATS2*, have been shown to develop soft-tissue sarcomas and ovarian stromal cell tumours (St. John *et al.* 1999). However, no reports on mice deficient in the *LATS2* gene have been shown.

Structural comparisons between mammalian Lats1 and Lats2 have revealed that the overall sequence similarity in the N-terminus between these proteins is much lower than in the kinase domain, except for two stretches of highly conserved sequence (Hori *et al.* 2000; Yabuta *et al.* 2000; Li *et al.* 2003). Therefore, the structural diversity or different modifications of the N-terminus between Lats1 and Lats2 are important to execute their independent functions during cell cycle. Enhanced expression of *LATS1* in human tumour cell lines caused cell cycle arrest at G_2/M through inhibition of Cdc2 kinase activity or induced apoptosis by up-regulating the level of pro-apoptotic proteins such as Bax or Caspase-3 (Yang *et al.* 2001; Xia *et al.* 2002). Moreover, Lats1 is phosphorylated in early prophase to function as a negative regulator of Cdc2 kinase by interacting with Cdc2 during mitosis (Tao *et al.* 1999) and is localized to the mitotic apparatus (Nishiyama *et al.* 1999; Hirota *et al.* 2000). Human *LATS2* is located at chromosome 13q11-12, in which a loss of heterozygosity has been frequently observed in many primary cancers (Yabuta *et al.* 2000). Over-expression of human Lats2/Kpm in HeLa cells has also shown to cause G_2/M arrest through inhibition of Cdc2 kinase activity and to induce apoptosis (Hori *et al.* 2000; Kamikubo *et al.* 2003), whereas over-expression of mouse Lats2 in *v-ras*-transformed NIH3T3 cells has shown to inhibit G_1/S transition through down-regulation of Cyclin E/Cdk2 kinase activity and to suppress tumorigenicity of NIH3T3/*v-ras* cells (Li *et al.* 2003). These observations suggest that Lats kinases act as tumour suppressors by inhibition of cell cycle progression or apoptosis. Although Lats1 was recently found to be phosphorylated by Cdc2 (Morisaki *et al.* 2002), the kinase that phosphorylates Lats2 has not yet been identified.

In this study, we show that Lats2 is phosphorylated by human Aurora-A kinase and that Lats2 and Aurora-A co-localize to the centrosome during the cell cycle. We also show that the Aurora-A-induced phosphorylation on Lats2 plays a role in its centrosomal localization.

Results

Lats2 is phosphorylated during the cell cycle

Lats2 has been reported to be phosphorylated in the M phase (Hori *et al.* 2000). We therefore examined, here, the phosphorylation state of Lats2 during the cell cycle by arresting HeLa cells at the G_1/S phase by using the thymidine-aphidicoline double block method (Fig. 1A). Cells were harvested at the indicated times after the blocks had been removed and analysed by Western blotting with an anti-human Lats2 monoclonal antibody (3D10) (Yabuta *et al.* 2000). In synchronized cells, we observed that Lats2 migrated as two bands, one that migrated slowly and another that migrated more quickly. The slowly migrating band was particularly prominent in lysates of cells that had progressed to the M phase (8 h after release from the G_1/S phase). We also observed this band shift in the lysates of mitotic HeLa cells that had been treated by the microtubule-depolymerizing agent

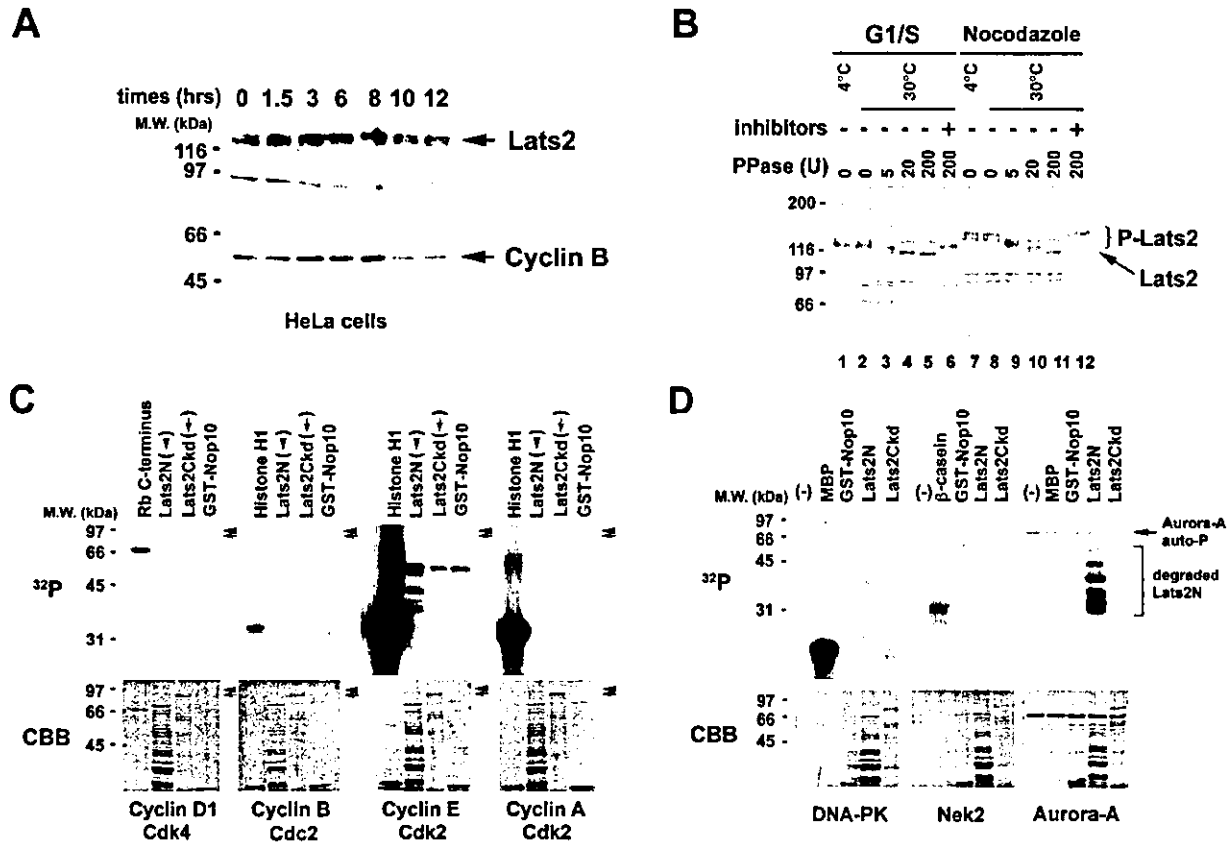

Figure 1 The phosphorylation of Lats2 is dependent on the cell cycle phase. (A) HeLa cells were arrested in the G_1/S phase by the thymidine-aphidicoline double block method. Cells were released from the block by replacing the medium with fresh medium without drugs. Thirty micrograms of each extract prepared at the indicated time (h) after the release were analysed by Western blotting for Lats2 or Cyclin B. (B) HeLa cells were arrested in the G_1/S phase as time = 0 in A (left side) or the M phase by nocodazole-treatment (right side). The nuclear extract (Yabuta *et al.*, 2000) from each cell was incubated at 4 °C or 30 °C with the indicated concentrations (units) of lambda protein phosphatase (New England Biolabs) in the absence (–) or presence (+) of phosphatase inhibitors. These extracts were analysed by Western blotting with the 3D10 antibody. (C) Cyclin D1/Cdk4, Cyclin B/Cdc2, Cyclin E/Cdk2 and Cyclin A/Cdk2 kinase complexes purified from Sf-9 insect cells were used in *in vitro* kinase reactions. The substrates used were Rb C-terminus (for only Cyclin D1/Cdk4), Histone H1, GST-Lats2N (79–621), GST-Lats2Ckd (622-1088, kinase dead) or GST-Nop10 (as a negative control). These proteins were resolved by SDS–PAGE and ^{32}P-labelled proteins were visualized by autoradiography. The arrowheads and arrows indicate the locations of the GST-Lats2N (*c.* 96 kDa) and GST-Lats2C kDa (*c.* 86 kDa) proteins, respectively. Coomassie Brilliant Blue (CBB) staining shows a loading control (bottom panels). (D) An *in vitro* kinase reaction was performed with three different kinases and two Lats2 substrates. The kinases were GST-DNA-PK, GST-Nek2 and GST-Aurora-A. The substrates were GST-Lats2N (79–621) and GST-Lats2Ckd (622–1088, kinase dead). As a negative control substrate, GST-Nop10 was used. The proteins were resolved by SDS–PAGE and ^{32}P-labelled proteins were visualized by autoradiography. CBB staining shows a loading control (bottom panels).

nocodazole (Fig. 1B, lanes 7 and 8). To examine whether this band shift is due to phosphorylation of Lats2, nocozazole-treated HeLa cell lysates were incubated with various concentrations of lambda-protein phosphatase (Fig. 1B, lanes 9–11). The slowly migrating Lats2 band was converted into the fast-migrating band after the phosphatase treatment in a dose-dependent manner. This conversion was completely blocked by the addition of phosphatase inhibitors (Fig. 1B, lane 12), indicating that Lats2 is indeed phosphorylated at the M phase, in which nocodazole-treated cells are arrested by the spindle assembly checkpoint. Interestingly, we observed that the band corresponding to the Lats2 protein in the G_1/S-arrested cell lysates (the same sample as cell lysate of 0 h in Fig. 1A) was also converted by the phosphatase treatment into the fast-migrating band, which showed a similar mobility as the band in lane 11 of Fig. 1(B) (Fig. 1B, lanes 1–5). This conversion was also completely blocked by the addition of phosphatase inhibitors. These results indicate that Lats2 is phosphorylated not only at the M phase but also at the G_1/S phase. This G_1/S-phosphorylated band was also observed during interphase (Fig. 1A; 0, 1.5, 3, 10 and 12 h), indicating that Lats2 is phosphorylated during interphase. Therefore, these findings suggest that Lats2 is regulated by at least two distinct phosphorylation events during the cell cycle.

Lats2 is phosphorylated by Aurora-A *in vitro*

This cell cycle-dependent phosphorylation of Lats2 suggests that the regulation of Lats2 may be directly involved in cell cycle regulation. We wondered, therefore, whether the cell cycle-dependent phosphorylation of Lats2 could be mediated by the Cyclin/Cdk kinases. To test this notion, we performed *in vitro* kinase assays with four classes of Cyclin/Cdk kinases, namely, Cyclin D1/Cdk4, Cyclin B/Cdc2, Cyclin E/Cdk2 and Cyclin A/Cdk2, which act in G_1, G_2/M, G_1/S and S, respectively (Kitagawa *et al.* 1996). The substrates used were two truncated forms of glutathione-*S*-transferase (GST)-fused Lats2, namely, Lats2N (amino acids 79–621) and Lats2Ckd (amino acids 622–1088) (Fig. 2A) because full-length Lats2 was too unstable for recovery. We did not prepare the 1–78 amino acids region of Lats2 for a substrate of Cdk kinases because there is no consensus sequence of the Cdk phosphorylation site (S/T-P-X-R/K) (Kitagawa *et al.* 1996) in this region. GST-Lats2Ckd, which is defective in kinase activity due to the substitution of the catalytically essential lysine 687 residue with methionine (data not shown), was used rather than the intact Lats2C protein to prevent the autophosphorylation of Lats2C. As shown in Fig. 1(C), Cyclin D1/Cdk4 and Cyclin B/Cdc2 kinases could not phosphorylate either of the GST-Lats2 constructs, although these Cyclin/Cdk kinases could phosphorylate the substrates used as positive controls (Rb C-terminus or Histone H1). Although Cyclin E/Cdk2 and Cyclin A/Cdk2 appeared to slightly phosphorylate the degraded products of Lats2N, these may not be the major phosphorylation events to which Lats2 is subjected during the cell cycle because they are of similar intensity as the phosphorylation of the negative control substrate Nop10, which is a protein involved in the pseudouridylation of pre-rRNAs (Henras *et al.* 1998). These results suggest that the cell cycle-dependent phosphorylation of Lats2 is due to kinase(s) other than the Cyclin/Cdk kinases. In particular, it appears that the mitosis-dependent phosphorylation of Lats2 is not due to Cyclin B/Cdc2 kinase, which functions during mitosis.

As the kinase that phosphorylates Lats2 is not known, we searched for candidates with the *in vitro* kinase assay. When we tested DNA-PK (Kim *et al.* 1999), Nek2 (Fry *et al.* 1995) and Aurora-A, we found that only Aurora-A could phosphorylate Lats2N efficiently *in vitro* (Fig. 1D). Aurora A could not, however, phosphorylate GST-Lats2Ckd. Aurora-A is reported to be a centrosomal protein kinase whose kinase activities are regulated in a cell cycle-dependent manner (Nigg 2001) and peak at the G_2/M phase (Bischoff *et al.* 1998; Farruggio *et al.* 1999; Hirota *et al.* 2003).

Aurora-A kinase phosphorylates the serine 83 of Lats2 *in vitro*

To determine more specifically the region of Lats2 that is phosphorylated by Aurora-A, we produced several deletion mutants of Lats2 as GST-fusion proteins (Fig. 2A) and used them as substrates in the *in vitro* kinase assay. As shown in Fig. 2(B), GST-Lats2 proteins containing amino acids 1–118, 79–118, 79–151, 79–257 and 79–621 were readily phosphorylated by Aurora-A, whereas the Lats2 proteins consisting of amino acids 1–78 and 113–151 were very poorly phosphorylated. This suggests that Aurora-A directly phosphorylates the amino acid 79–118 region of Lats2. To further map the Aurora-A phosphorylation site(s) on Lats2, we mutated serine 83 (S83), S91, threonine 93 (T93) or S94 in GST-79-118 to cysteine (S83C), cysteine (S91C), aspartic acid (T93D) or alanine (S94A), respectively. *In vitro* kinase assays with Aurora-A were performed with these mutated sequences. A loading control experiment with Coomassie Blue staining showed that an equal amount of each protein had been applied (Fig. 2C, right panel). Whereas phosphorylation of the S91C, T93D or S94A mutants was not significantly altered, the phosphorylation of the S83C mutant was remarkably diminished (Fig. 2C,

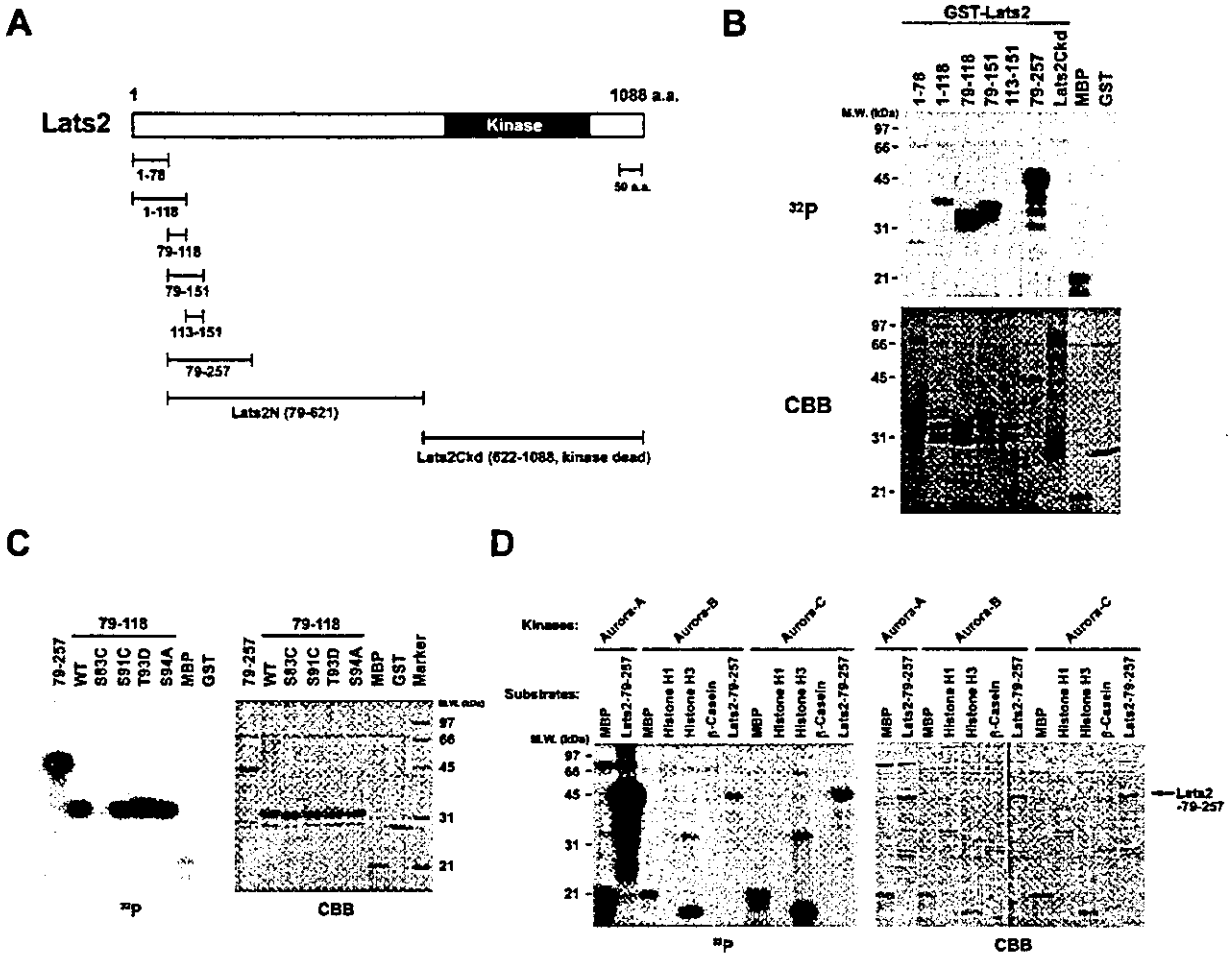

Figure 2 Recombinant Aurora-A kinase phosphorylates the S83 residue of Lats2 *in vitro*. (A) Schematic diagram of Lats2 that shows the location of the kinase domain. Beneath are the GST-fusion proteins used in the kinase reactions, namely, those containing Lats2 amino acids 1–79, 1–118, 79–118, 79–151, 113–151, 79–257, 79–621 (Lats2N) and 622–1088 (Lats2Ckd, kinase dead). (B) *In vitro* kinase reactions were performed with GST-Aurora-A and truncated GST-Lats2 proteins. The truncated GST-fusion proteins used were those containing amino acids 1–78, 1–118, 79–118, 79–151, 113–151, 79–257 and 622–1088 (Lats2Ckd) of Lats2. CBB staining shows a loading control (bottom panel). (C) An *in vitro* kinase reaction was performed with GST-Aurora-A and GST-Lats2-79-118 proteins that harbour the indicated substitutions (left panel). CBB staining shows that equal amounts of proteins were present (right panel). (D) *In vitro* kinase reactions were performed using GST-Lats2-79-257 as a substrate with the kinases GST-Aurora-A, GST-Aurora-B and GST-Aurora-C. CBB staining shows a loading control (right panel).

left panel). In addition, we found that the S83 residue is conserved not only in human Lats2 but also in mouse Lats2, mouse Lats1 and human Lats1 (data not shown). We also asked whether Aurora-B and -C can phosphorylate Lats2 as well as Aurora-A. An *in vitro* kinase assay was performed with these purified Aurora kinases using purified Lats2-79-257 as a substrate. Lats2 was phosphorylated by Aurora-B and -C but much more inefficiently than Aurora-A (Fig. 2D). These results indicate that Lats2, at least the 79–257 region, is phosphorylated predominantly by Aurora-A and weakly by Aurora-B and Aurora-C *in vitro*.

Aurora-A kinase phosphorylates the serine 83 of Lats2 *in vivo*

To confirm that S83 of Lats2 is phosphorylated by Aurora-A, we raised a specific monoclonal mouse anti-phospho-S83 antibody (3B11) by immunizing mice with a Lats2 peptide whose S83 residue is phosphorylated. The *in vitro* kinase assay was performed with wild-type Aurora-A or the kinase-dead form of Aurora-A with GST-Lats2-79-118 (WT) or GST-Lats2-79-118 (S83C) in the absence of [γ-^{32}P]ATP and analysed by Western blotting with the 3B11 antibody (Fig. 3A). When wild-type

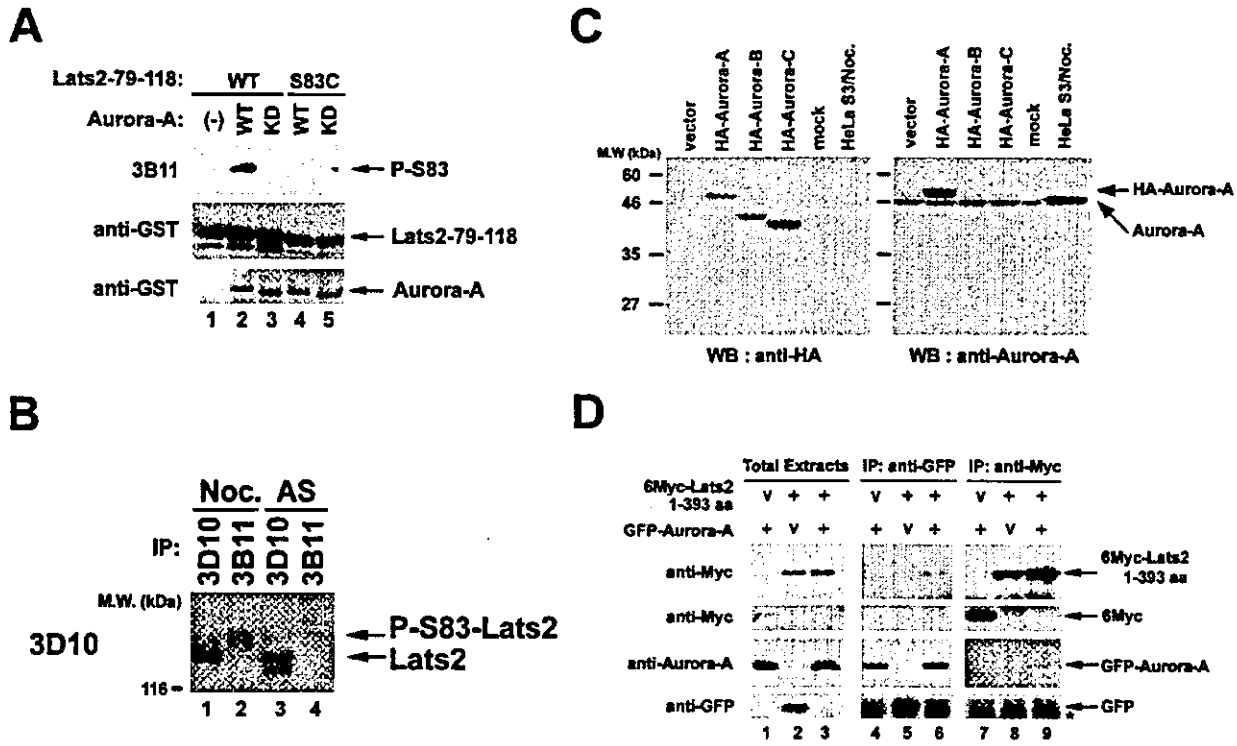

Figure 3 Lats2 is phosphorylated on S83 and interacts with Aurora-A *in vivo*. (A) Specificity of the anti-phospho-S83 monoclonal antibody (3B11). *In vitro* kinase reactions were performed with GST-Lats2-79-118-WT (lanes 1–3) or -S83C (lanes 4 and 5) using GST-Aurora-A (WT; lanes 2 and 4) or GST-Aurora-A-kinase-dead (KD; lanes 3 and 5) in the absence of [γ-^{32}P]ATP. The assays were analysed by Western blotting with the 3B11 antibody (top panel). That equal amounts of GST-Lats2-79-118 or GST-Aurora-A proteins were present was confirmed by Western blotting with anti-GST antibody (middle and bottom panels). (B) Phosphorylation state of endogenous Lats2 protein at the M phase. Endogenous Lats2 was immunoprecipitated from nocodazole-arrested M phase (Noc.) or asynchronous (AS) cell extracts with the anti-Lats2 monoclonal antibody (3D10; lanes 1 and 3) or the anti-phospho-Ser83 monoclonal antibody (3B11; lanes 2 and 4), followed by Western blotting with the 3D10 antibody. (C) Specificity of the anti-Aurora-A polyclonal antibody. 293T cells were transfected with HA-tagged Aurora-A, Aurora-B, Aurora-C or vector alone. The whole cell lysates were resolved by SDS-PAGE, followed by Western blotting with anti-HA (left panel) or anti-Aurora-A antibodies (right panel). (D) *In vivo* interaction of Lats2-1-393 with Aurora-A. 293T cells were co-transfected with 6Myc-Lats2-1-393 (lanes 2, 3, 5, 6, 8 and 9) and/or GFP-Aurora-A (lanes 1, 3, 4, 6, 7 and 9). As controls, the lysate of 293T cells transfected with empty vectors were used (V; lanes 1, 2, 4, 5, 7 and 8). GFP-Aurora-A or 6Myc-Lats2-1-393 was immunoprecipitated with the anti-GFP antibody (lanes 4–6) or anti-Myc antibody (lanes 7–9), respectively. Whole cell lysates (lanes 1–3, about 7 μg each) and immunoprecitates were resolved by SDS-PAGE, followed by Western blotting with the anti-Myc (top and 2nd panels from top) or anti-Aurora-A (3rd panel from top) or anti-GFP antibodies (bottom panel). An asterisk indicates IgG light chain.

Aurora-A was used, the 3B11 antibody specifically detected the phosphorylated form of WT Lats2-79-118 (lane 2). However, no phosphorylation of the S83 site was detected when kinase-dead Aurora-A was used (lane 3). Therefore, the 3B11 antibody is specific for the phosphorylated form of S83.

The 3B11 antibody was used to show that the S83 residue in endogenous Lats2 is phosphorylated *in vivo* in a cell cycle-dependent manner. The 3D10 antibody that recognizes Lats2 was also used. Therefore, the Lats2 proteins in lysates from nocodazole-treated or asynchronous HeLa cells were immunoprecipitated with either the 3D10 or the 3B11 antibody, followed by Western blotting using the 3D10 antibody (Fig. 3B). The 3B11 antibody immunoprecipitated the phosphorylated-S83-Lats2 protein from the nocodazole-treated cell lysate (lane 2) but not from the asynchronous cell lysate (lane 4). In contrast, the 3D10 antibody brought down equivalent amounts of Lats2 protein from each cell lysate (lanes 1 and 3), although the 3D10 antibody could not recognize the M phase-specific phosphorylated form of Lats2 in the immunoprecipitate of the 3D10 antibody (lane 1). The 3D10 antibody may be able to recognize the M phase-specific phosphorylated form of Lats2 in Western

blotting but not to immunoprecipitate it under this experimental condition. Therefore, the S83 residue in endogenous Lats2 is the primary phosphorylation site *in vivo*. Taken together, we conclude that Aurora-A is the phosphorylating kinase of Lats2 in the M phase because Aurora-A predominately phosphorylates S83 on Lats2 *in vitro* and this site is also phosphorylated *in vivo*.

Lats2 interacts with Aurora-A

Next, we raised a polyclonal rabbit antibody against GST-Aurora-A protein. 293T cells expressing HA-tagged Aurora-A, -B, -C or vector alone were lysed and analysed by Western blotting with either anti-Aurora-A (Fig. 3C, left panel) or anti-HA (right panel) polyclonal antibody. The anti-Aurora-A antibody specifically recognized only HA-Aurora-A but not HA-Aurora-B or HA-Aurora-C. In addition, the anti-Aurora-A antibody also recognized a band corresponding to the endogenous Aurora-A protein in 293T cells and untransfected HeLa S3 cells. Therefore, it appears that the anti-Aurora-A antibody specifically recognizes the Aurora-A protein and does not crossreact with other proteins. Using this antibody, we performed co-immunoprecipitation experiments to know whether Aurora-A and Lats2 interact *in vivo*. As we were unable to confirm the interaction of endogenous Aurora-A with Lats2 by immunoprecipitation assays using anti-Aurora-A or 3D10 antibodies (data not shown), we co-transfected 293T cells with GFP (green fluorescent protein)-Aurora-A and/or 6Myc-Lats2-1-393 (Fig. 3D, lanes 1–3). When we performed immunoprecipitation experiments with each transfected cell extract by using the anti-GFP antibody, we detected 6Myc-Lats2-1-393 in the GFP-Aurora-A immunoprecipitate (Fig. 3D, top panel, lane 6). In reciprocal immunoprecipitation experiments, GFP-Aurora-A was detected in the 6Myc-Lats2-1-393 immunoprecipitate (Fig. 3D, third panel from top, lane 9). This weak interaction between Lats2 and Aurora-A is reminiscent of an unstable complex that is commonly observed between an enzyme and a substrate. These results indicate that Aurora-A interacts with the N-terminus (1–393 amino acids) of Lats2 *in vivo*, which supports the notion that Lats2 is a phosphorylation target of Aurora-A *in vivo*.

Lats2 co-localizes with Aurora-A at the centrosome

If Lats2 is a phosphorylation target of Aurora-A *in vivo*, it is likely that their subcellular distributions are similar during the cell cycle. To test this possibility, we examined whether Lats2 co-localizes with Aurora-A during various cell cycle stages. As the 3D10 antibody, which was raised against the N-terminal portion (amino acids 78–256) of Lats2, could not detect any endogenous Lats2-specific signals, HeLa S3 cells were transiently transfected with GFP-fused full-length human Lats2 or the GFP-vector alone, followed by immunofluorescence staining with anti-Aurora-A antibody (Fig. 4A). GFP-Lats2 was observed as one or two bright spots beside the nucleus in interphase (left panels, i and ii; green). In prophase, these bright spots translocated toward the opposite poles of the cell (left panel, iii). A similar pattern was also observed for Aurora-A, except that Aurora-A was located within the nucleus (middle panels; red). The nuclear localization of Aurora-A was detected with both of the anti-Aurora-A antibodies and we observed no signal with the secondary antibody alone in our experiments (data not shown). Therefore, it is unlikely that the localization of Aurora-A in the nucleus as determined by these two antibodies is as a result of cross-reaction of anti-Aurora-A antibodies. The yellow spots in the merged images indicate that GFP-Lats2 co-localizes with Aurora-A during interphase, prophase and telophase (right panels). However, when the cells enter metaphase, the GFP-Lats2-specific signal was diffusely distributed throughout the cell (left panel, iv), whereas Aurora-A was localized to two predominant bright spots that are reminiscent of the spindle microtubules and the spindle poles. A similar change in subcellular distribution was also observed in the cells expressing the 6Myc-tagged Lats2 construct (Fig. 4B,i and C,i and ii), and the diffuse distribution of Lats2 was also observed during anaphase (Fig. 4B,ii). Interestingly, when cells enter cytokinesis, GFP-Lats2 was observed again as bright spots and the spots were distributed to daughter cells and localized at each pole (Fig. 4A,v), which is suggestive of re-localization to the centrosomes of GFP-Lats2 when the cells enter cytokinesis. Moreover, GFP-Lats2 was also found at the midbody during cytokinesis (Fig. 4A,v). Together with the previous reports that Aurora-A is localized to the interphase and mitotic centrosomes as well as to the spindle poles (Bischoff *et al.* 1998; Zhou *et al.* 1998), these results indicate that Lats2 co-localizes with Aurora-A at the centrosomes during interphase, early prophase and cytokinesis. That Lats2 localizes to centrosomes during interphase was also confirmed by its co-localization with γ-tubulin (Fig. 4C).

The S83 of Lats2 is phosphorylated at the centrosome, the mitotic spindle pole and the midbody

To confirm that S83 on Lats2 is phosphorylated at the centrosomes *in vivo*, the spatial and temporal distributions

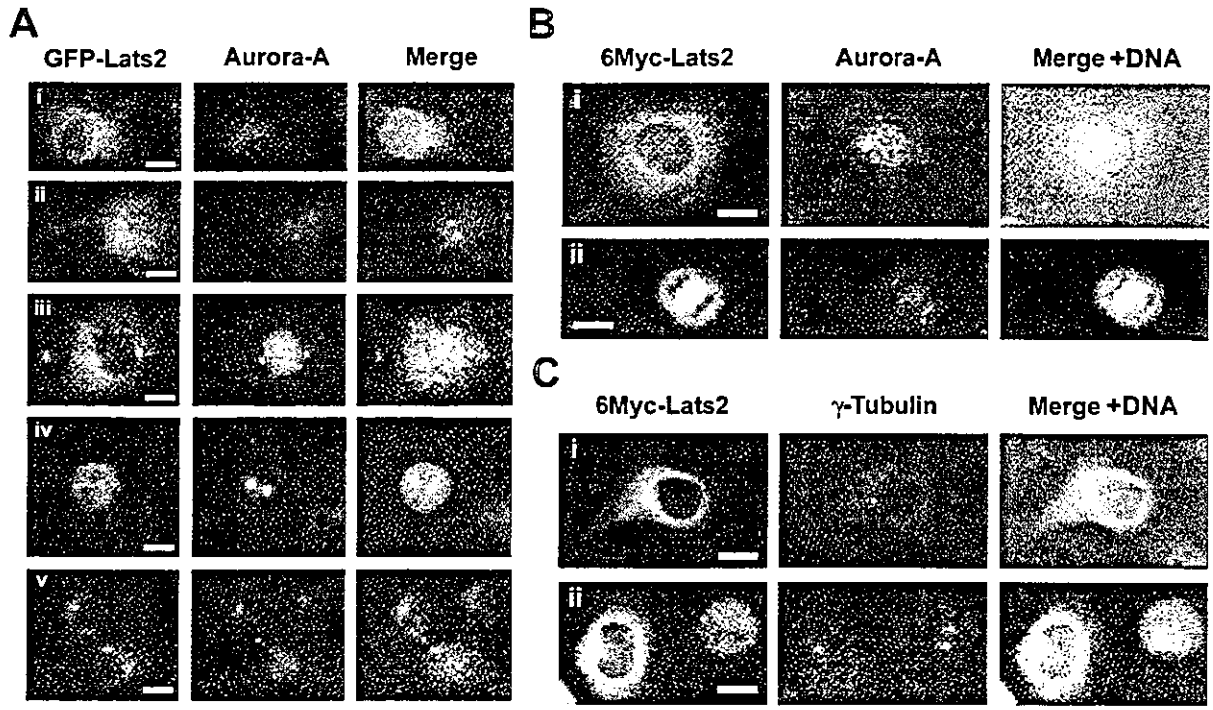

Figure 4 Lats2 co-localizes with Aurora-A at the centrosome. HeLa S3 cells were transiently transfected with GFP-fused full-length Lats2 (A) or 6Myc-tagged full length Lats2 (B and C). The transfected cells were synchronized at the S phase by thymidine-single block, released from the block and then fixed with formaldehyde at various cell cycle stages: interphase (A-i, -ii, B-i and C-i), prophase (A-iii), metaphase (A-iv and C-ii), anaphase (B-ii) and telophase (A-v). 6Myc-Lats2 was visualized by immunofluorescence staining of the fixed cells with anti-Myc antibody followed by incubation with Alexa-Fluor 488-conjugated anti-mouse immunoglobulin G (B and C, green). Aurora-A or centrosomes were visualized by immunofluorescence staining with anti-Aurora-A (A and B, red) or anti-γ tubulin (C, red) antibody, respectively, followed by Texas Red or Alexa-Fluor 594-conjugated anti-rabbit immunoglobulin G. DNA was visualized by staining with Hoechst 33258 (B and C, blue). DNA and merged images are shown in the right panels. The yellow signals reflect the co-localization of GFP- or 6Myc-tagged Lats2 and the indicated proteins (Aurora-A or γ-tubulin). Scale bar, 10 μm.

of the S83-phosphorylated (pS83) Lats2 in HeLa S3 cells were analysed with the 3B11 antibody. As shown in Fig. 5(A), the phosphorylation signals of S83 by the 3B11 antibody were observed at the centrosomes of interphase and prometaphase cells (Fig. 5A,i and ii, left panels) and at the spindle poles of metaphase, anaphase and telophase cells (Fig. 5A,iii,iv and v, left panels). The centrosomal localization of pS83 was also confirmed by its co-localization with γ-tubulin (Fig. 5A,i–vi, right panels; yellow). The S83-phosphorylations of endogenous Lats2 and the subcellular localizations of GFP- and 6Myc-tagged Lats2 were observed at both a single centrosome and duplicated centrosomes during interphase (Figs 4 and 5, and data not shown). Centrosomes are duplicated during early S phase and mature during late S phase. Centrosomes then separate during early mitosis (reviewed in Doxsey 2001; Nigg 2002). Therefore, these results suggest that both the centrosomal localization and the initial S83-phosphorylations of Lats2 occur before S phase. The S83-phosphorylations at the centrosomes or the spindle poles were more prominent at prometaphase and metaphase (Fig. 5 and B,ii and iii, green spots) than at the other stages. These observations are similar to the subcellular localization of Aurora-A during the cell cycle (Fig. 5B). However, Aurora-A localizes to both the spindle poles and half-spindles, while the S83-phosphorylated Lats2 localizes only to the spindle poles during mitosis. Interestingly, during cytokinesis, while the S83-phosphorylation disappeared from the centrosomes or the spindle poles, it was detected at the midbody (Fig. 5A,vi and 5B-vi, left panels). It is noteworthy that this localization of pS83 during cytokinesis is more similar to that of Aurora-B than Aurora-A (Crosio *et al.* 2002). These results suggest that the endogenous Lats2 is localized to the centrosomes/the spindle poles, where it is phosphorylated on S83 by Aurora-A during the cell cycle.

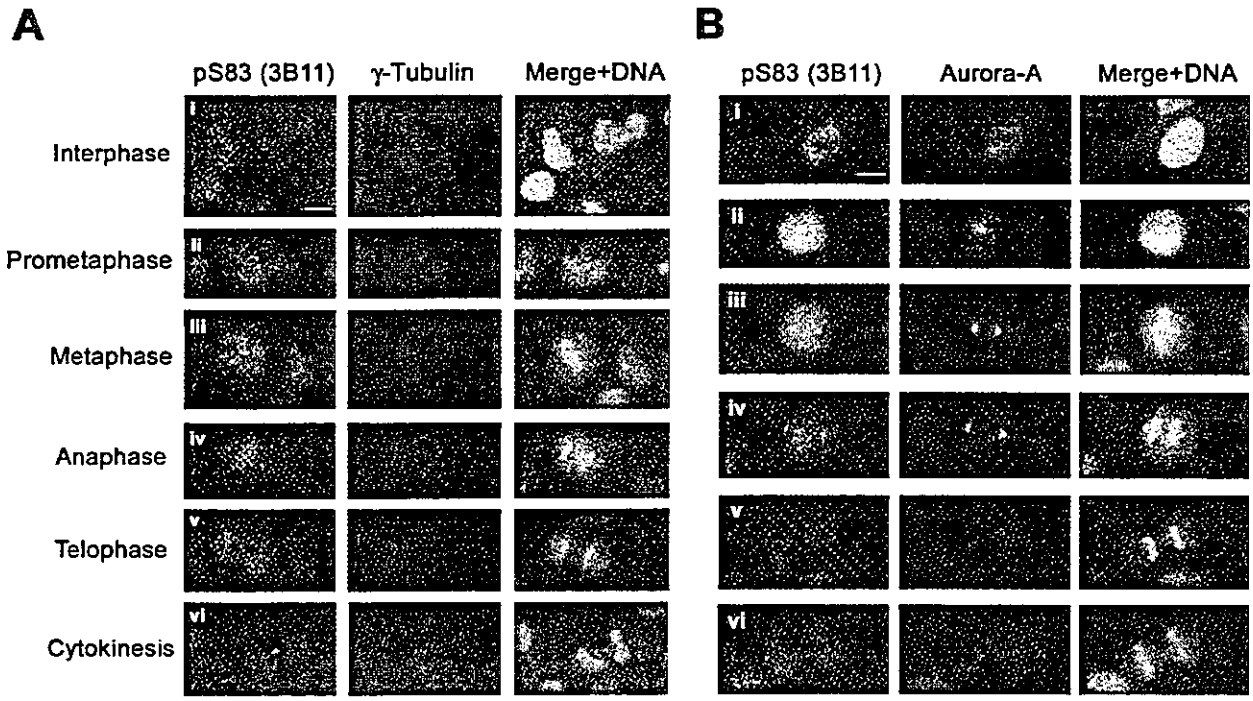

Figure 5 S83-phosphorylated Lats2 localizes to the centrosomes/spindle poles during the cell cycle besides cytokinesis. (A and B) HeLa S3 cells were synchronized at the S phase by thymidine-single block, released from the block and then fixed with formaldehyde at interphase (i), prometaphase (ii), metaphase (iii), anaphase (iv), telophase (v) and cytokinesis (vi). S83-phosphorylated Lats2 was visualized by immunofluorescence staining with the 3B11 antibody followed by incubation with Alexa-Fluor 488-conjugated anti-mouse immunoglobulin G (left panels, green). Centrosomes/spindle poles or Aurora-A were respective visualized with anti-γ-tubulin (A) or anti-Aurora-A (B) antibodies (2nd panels from left, red). DNA was visualized by staining with Hoechst 33258 (blue). DNA and merged images are shown in the right panels. The yellow signals indicate the co-localization of S83-phosphorylated Lats2 with the centrosomes/spindle poles. Scale bar, 10 μm.

Phosphorylation of S83 plays a role of the centrosomal localization of Lats2

To explore the significance of S83 phosphorylation in Lats2 localization, HeLa S3 cells were transfected with 6Myc-tagged full-length human Lats2 containing S83C or S83E (S83 mutated to glutamate), and the centrosomes were detected by staining with γ-tubulin (Fig. 6A and B, 2nd panels from left, red). The subcellular localization of both the S83C and S83E mutants during the cell cycle frequently showed mislocalization of Lats2 at the centrosome(s) of interphase HeLa S3 cells (Fig. 6A and B, top-left panel, arrows) in comparison with the 6Myc-Lats2 wild-type (Figs 4C and 6A and B; these experiments were performed in equal conditions). In mitotic cells, there is no detectable staining of the S83 mutant proteins (S83C, S83E) (Fig. 4A and B, bottom-left panels), as well as wild type (Fig. 4C). Therefore, we could not obtain any data on the centrosomal localization by comparison between each S83 mutant and wild type during all phases of mitosis. Next, among the cells expressing each 6Myc-Lats2 -WT, -S83C or -S83E, the numbers of cells in which the 6Myc-Lats2 obviously localized to the centrosome(s) during interphase were counted to assess the percentages of the centrosomal localization of Lats2 WT and two S83 mutants. As shown in Fig. 6(C), in 55% of cells expressing Lats2 WT, the 6Myc-Lats2 localized to the centrosome while, in the case of the S83C and S83E mutants, the percentage of cells harbouring the centrosomal Lats2 were reduced by less than 30 and 43%, respectively. These results indicate that the non-phosphorylation of the Ser 83 residue disturbs the centrosomal localization of Lats2.

Discussion

In this study, we have shown that Lats2 is phosphorylated in at least two distinct stages of the cell cycle, G_1/S phase and M phase containing nocodazole arrest (Fig. 1A and B), suggesting that Lats2 is regulated by multiple

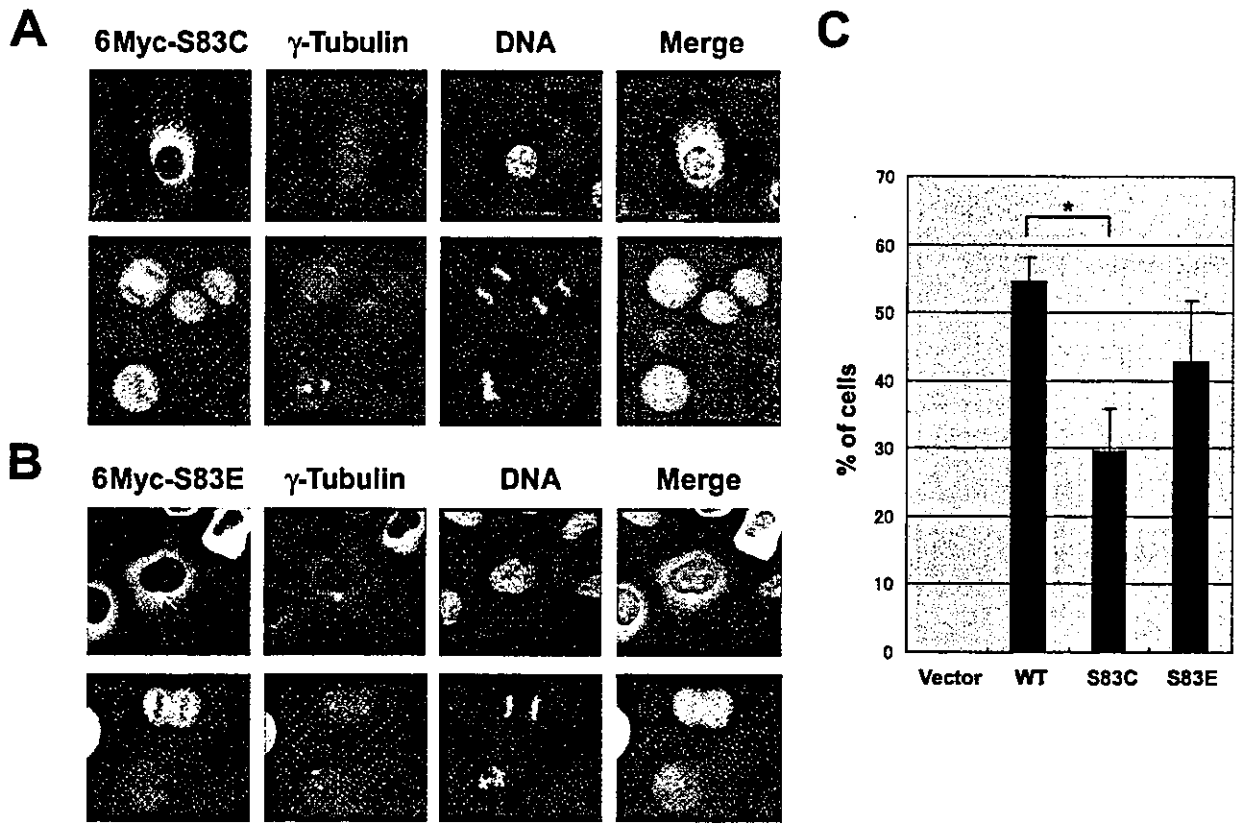

Figure 6 The phosphorylation of S83on Lats2 plays a role of its centrosomal localization. HeLa S3 cells were transiently transfected with 6Myc-tagged full-length Lats2-S83C (A) or 6Myc-tagged full-length Lats2-S83E (B). The transfected cells were fixed with formaldehyde at interphase (A-top and B-top panels), prometaphase (lower in B-bottom panel), metaphase (lower in A-bottom panel), anaphase (upper left in A-bottom panel) and telophase (upper right in A-bottom panel). 6Myc-Lats2 was visualized by immunofluorescence staining of the fixed cells with anti-Myc antibody followed by Alexa-Fluor 488-conjugated anti-mouse immunoglobulin G (A and B, green). Centrosomes were visualized by immunofluorescence staining with anti-γ-tubulin antibody (A and B, red), followed by Alexa Fluor 594-conjugated anti-rabbit immunoglobulin G. The positions of centrosomes are indicated by white arrows. DNA was visualized by staining with Hoechst 33258 (A and B, blue). Merged images are shown in the right panels. The yellow signals reflect the co-localization of the 6Myc-Lats2 proteins and γ-tubulin. (C) Histogram shows the percentages of cells in which the indicated 6Myc-tagged proteins localize to the interphase centrosomes in HeLa S3 cells. These results were obtained from four independent experiments (more than 50 positive cells in 500 cells each) and bars indicate standard deviations. All data were statistically analysed based on the Student's *t*-test. $*P = 0.001$.

phosphorylations throughout the cell cycle. Cyclin E/Cdk2 and Cyclin A/Cdk2 kinases alone could produce very weak phosphorylation signals on the degradation products of Lats2N (Fig. 1C). This observation might suggest that one of the phosphorylated forms of Lats2 during interphase may be due to Cyclin E/Cdk2 and Cyclin A/Cdk2 kinases. Because it is probable that mouse Lats2 also regulates the G_1/S transition through down-regulation of Cyclin E/Cdk2 kinase activity in NIH3T3 cells (Li *et al.* 2003), the G_1/S-dependent phosphorylation(s) of Lats2 that we have shown in Fig. 1(B) may be implicated in some functions of Lats2 on G_1/S transition. We identified a centrosomal kinase, Aurora-A, as one of the candidate kinases for phosphorylation of S83 residue on Lats2. Immunostaining data with the anti-phosphorylated S83 antibody reveals that S83 on Lats2 is phosphorylated *in vivo* during the cell cycle and it is more prominent during prophase and metaphase than interphase, anapahse and telophase, which is similar to the expression pattern of Aurora-A during the cell cycle (Fig. 4A and Bischoff *et al.* 1998). These results suggest that S83 on Lats2 is a phosphorylation target of Aurora-A *in vivo*. As Aurora-B and -C also phosphorylate Lats2, although very weakly (Fig. 2D), it will be important to examine in future whether Aurora-B or Aurora-C can more efficiently phosphorylate S83 or

other sites of Lats2 by using the full-length protein of Lats2. In fact, subcellular localization of phosphorylated S83 is observed at the midbody of cytokinesis cells, which is similar to that of Aurora-B (Fig. 5). Therefore, the phosphorylation of S83 on Lats2 may be regulated by not only Aurora-A but also Aurora-B.

Immunofluorescence data of exogenous GFP or 6Myc-tagged Lats2 protein indicate that Lats2 and Aurora-A co-localize at the centrosome during the cell cycle, except for metaphase and anaphase. We previously showed that Lats2 exists in the 'nuclear fraction' that was prepared from cell lysates by Western blot analysis (Yabuta *et al.* 2000). Probably, the centrosome was distributed in this fraction during our subfractionation procedure. Although a recent report of Li *et al.* has shown that ectopically expressed mouse Lats2 localized in the cytoplasm of NIH3T3 cells and that the majority of endogenous Lats2 protein is located in the cytoplasm in their fractionation experiments using lung cancer cells (Li *et al.* 2003). Moreover, the ectopic over-expression of Lats2 in cells tends to localize diffusely to the cytoplasm (Figs 4 and 6), which may be due to the degradation of exogenous Lats2 protein. However, our immunostaining data using the 3B11 antibody showed that endogenous Lats2 protein is located not only at centrosomes but also in the nucleus during interphase (Fig. 5A,i and B,i). These observations are consistent with the previous reports that Aurora-A localizes to both the centrosome and the nucleus during the G_2 phase (Crosio *et al.* 2002; Hirota *et al.* 2003). Recently, Aurora-A was reported to be required for mitotic entry of human cells in concert with its interacting activator Ajuba, a LIM protein. It is likely that Aurora-A is initially activated at the G_2 phase and its activity is required for the recruitment of the Cyclin B1/Cdc2 complex to centrosomes (Hirota *et al.* 2003). Although Lats2 localized to the centrosome before its duplication in early S phase, it is not possible that Lats2 is involved in the regulation of centrosomal duplication, because we could also observe two close spots of γ-tubulin, as well as typical and normal duplications of the centrosome, in HeLa cells in which the wild-type or the S83 mutants of Lats2 was over-expressed ectopically. Moreover, in accordance with a previous report on a role of *Drosophila* Aurora-A in centrosome maturation, Aurora-A promotes the recruitment of D-TACC to centrosomes and phosphorylates it (Giet *et al.* 2002). Because the phosphorylation of S83 on Lats2 is one of requirements for centrosomal localization of Lats2 in this issue, Aurora-A may also promote the recruitment of Lats2 to centrosomes as well as Cyclin B1/Cdc2 complex and D-TACC for the centrosome maturation. The accumulated Lats2 kinase at the centrosome may rapidly phosphorylate other centrosomal components, together with some centrosomal kinases including Cdc2 and Plk1, polo-like kinase, in order to progress the centrosome maturation efficiently. γ-Tubulin is one of the components that are recruited to the MTOC (microtubule-organizing centre) during the centrosome maturation. When the wild-type or the S83 mutants of Lats2 were over-expressed in HeLa cells, we could observe one or two spots of γ-tubulin in these cells (Figs 4 and 6), which is suggestive of the recruitment of γ-tubulin to MTOC. Therefore, it is unlikely that Lats2 is involved, at least in the recruitment of γ-tubulin. Moreover, the over-expression of the wild-type or the S83 mutants of Lats2 did not cause abnormal chromosome alignment and aberrant mitotic spindle formation (Figs 4 and 6, and data not shown). To date, several structurally different protein kinases, including Aurora kinases and Cdks, have been shown to localize at the centrosome regulating the centrosomal function during the cell cycle (Mayor *et al.* 1999). Among these proteins, Nek2, as a NIMA-like kinase and Plk1 are representative centrosomal kinases, although Nek2 could not phosphorylate Lats2 *in vitro*. Although as yet untested, it is intriguing whether Plk1 also phosphorylates Lats2 because Plk1 is involved in not only controlling centrosomal functions but also DNA damage checkpoint (Smits *et al.* 2000). However, the GFP-Lats2 or 6Myc-Lats2-specific signal was diffusely distributed throughout the cell but not at the centrosome during mitosis (Fig. 4). By using the 3B11 antibody, we could observe that endogenous Lats2 localizes at the centrosome or the spindle pole during mitosis. Therefore, the diffusely distribution of GFP- and 6Myc-Lats2 may also be due to the effects of over-expression of these proteins in a mitotic cell, including the protein degradation.

When the kinase activities of these Lats2 mutants were assessed by examining the auto-phosphorylation of immunoprecipitates generated by the anti-GFP antibody from extracts expressing GFP-Lats2 wild-type or S83C mutant, we were unable to observe remarkable differences in their phosphorylation levels (data not shown). A previous report has shown that over-expression of either wild-type or kinase inactive form of Aurora-A in HeLa cells triggered mitotic defects including aberrant cytokinesis and the formation of tetraploid cells, but not centrosome amplification in S phase (Meraldi *et al.* 2002). Therefore, we suppose that the Aurora-A-dependent phosphorylation of S83 on Lats2 is not implicated in the aberrant cytokinesis and the formation of tetraploid cells caused by over-expression of Aurora-A in HeLa cells. On this issue, we showed that S83 phosphorylation plays a role of the centrosomal localization of Lats2 (Fig. 6). It

is noteworthy that there is no detectable staining of the S83 mutant proteins in telophase cells, although this is seen in cells expressing the wild-type protein (Fig. 6A and B). Therefore, it can be speculated that the phosphorylation of S83 may be involved in not only its centrosomal localization but also its midbody localization during cytokinesis. Moreover, we showed that all of the cells expressing S83C mutant are not localized to the centrosome (Fig. 6C). The result suggests that the phosphorylation of S83 is not the only cause for centrosomal localization of Lats2 and therefore further studies are required. Recently, a report has shown that Lats2 kinase activity and two LATS conserved domains (LCD1 and LCD2), two stretches of highly conserved sequence in amino-terminus between Lats1 and Lats2, are required for Lats2 to suppress tumorigenicity and to inhibit cell proliferation (Li *et al.* 2003). It is notable that S83 locates in LCD1. The phosphorylation of S83 by Aurora-A may be important for Lats2 to suppress tumorigenicity and to inhibit cell proliferation via centrosomal regulations.

Taken together, our data suggest that Lats2 is a novel centrosome-associated kinase that may be involved in regulating the centrosome and/or mitotic spindle downstream of Aurora-A.

Experimental procedures

Cell culture, cell cycle synchronization and transfections

All cell lines were maintained in Dulbecco's modified Eagle's medium (DMEM) with 10% foetal calf serum (FCS, HyClone, Logan, UT, USA), 100 U/mL penicillin and 100 μg/mL streptomycin. HeLa cells were synchronized to enter the G_1/S phase by the thymidine-aphidicoline double block and release protocol (Tsuruga *et al.* 1997). Cells at the G_2/M phase were collected 9 h after release. Mitotic cells were only obtained by shaking-off after incubation for 18 h in medium containing 80 ng/mL nocodazole. Cell synchrony was monitored by Western blotting with anti-Cyclin B antibody or by FACS analysis (Becton-Dickinson, Franklin Lakes, NJ, USA). Transient transfection of HeLa S3 and 293T cells were carried out using LipofectAMINE or PLUS reagents according to the manufacturer's instructions (Invitrogen, Carlsbad, CA, USA).

Plasmids and site-directed mutagenesis

To isolate the complete human *LATS2* cDNA, we screened a human placenta cDNA library (Clontech), using as a probe *Hin*dIII-*Pst*I fragments from the pAP3neo-*HsLATS2* plasmid that contains partial Lats2 cDNA (Yabuta *et al.* 2000). The nucleotide sequences of both strands of the isolated clone were determined by the dideoxy chain termination method. To construct the pCMVmyc-Lats2 full plasmid, we prepared *Bam*HI-*Xcm*I fragments by polymerase chain reaction (PCR) using the isolated clone as a template. These fragments were inserted into the *Bam*HI and *Xcm*I sites of the pCMV-*HsLATS2* plasmid (Yabuta *et al.* 2000). For expression in bacteria, full Lats2 cDNA was released from the pCMVmyc-Lats2 full plasmid by *Bam*HI and *Xho*I cleavage and recloned into the pGEX4T vector to produce pGEX4T-Lats2 (Amersham Pharmacia Biotech, Piscataway, NJ, USA). pGEX-Lats2N was constructed by ligating the *Eco*RI-*Hpa*I fragment from pAP3neo-*HsLATS2* into *Eco*RI and *Sma*I sites of pGEX4T2. pGEX-Lats2C was constructed by ligating the *Bam*HI-*Xho*I fragment from another plasmid, pCMVmyc-Lats2C, into the *Bam*HI and *Xho*I sites of pGEX4T. The pCMVmyc-Lats2C plasmid had been constructed by ligating the *Hinc*II-*Not*I fragment from pAP3neo-*HsLATS2* into the *Eco*RV and *Not*I sites of pCMVmyc. pGEX-Lats2-79-257 was constructed by digesting pGEX-Lats2N with *Not*I followed by self-ligation. pCMV6myc-Lats2 full was constructed by ligating the *Bam*HI-*Xho*I fragment from pCMVmyc-Lats2 full into the *Bam*HI and *Xho*I sites of pCMV6myc. pCMV6myc-Lats2-1-393 was constructed by ligating the *Bam*HI-*Pml*I fragment from pGEX-Lats2 into the *Bam*HI and *Eco*RV sites of pCMV6myc. The other truncated Lats2 mutants were constructed in pGEX4T by PCR with the following primers which contain either an *Eco*RI site or a *Xho*I site: Lats2-1-78, F11 (5′-CCGGAATTCATGAGGCCAAAGAGTTTTCCT-3′) and R9 (5′-ATACTCGAGCCTCAAGGCTTTCTGATAAGG-3′); 1-118, F11 and R3 (5′-ATACTCGAGGCCAGCCATCTCCTGGTC-3′); 79-118, F2 (5′-GCGGAATTCGAAATCAGATAT TCCTTGTTG-3′) and R3; 79-151, F2 and R2 (5′-ATACTCGAGCGCACAATCTGCTCATTCC-3′); 113-151, F3 (5′-ATAGAATTCGACCAGGAGATGGCTGGC-3′) and R2. All point mutants of Lats2 and Aurora-A KD (kinase dead: D273E) (Shindo *et al.* 1998) were generated by site-directed mutagenesis using the QuickChange Site-Directed Mutagenesis Kit (Stratagene, La Jolla, CA, USA) according to the manufacturer's instructions. Aurora-A (Aik2) (Zhou *et al.* 1998), Aurora-B (AIM1) (Tatsuka *et al.* 1998) and Aurora-C (AIE2) (Tseng *et al.* 1998) cDNA were generated by PCR from the human placenta cDNA library. All amplified sequences were confirmed by DNA sequencing.

Expression and purification of recombinant proteins

For the expression of GST-fused Lats2 mutants, Aurora-A, Aurora-B, Aurora-C and Aurora-A KD, pGEX plasmids with the appropriate cDNAs were introduced into bacteria. The cultures were induced with 0.5 mM isopropyl β-D-thiogalactopyranoside (IPTG) and incubated at 37 °C for 6 h. Cells were collected and lysed in PBS containing 1% Triton X-100, 2 μg/mL leupeptin, 10 μg/mL aprotinin, 1 mM PMSF, 1 mM benzamidine, 1 mM NaF and 1 mM Na_3VO_4 by brief sonication. After centrifugation, the clear lysate was adsorbed to Glutathione Sepharose 4B (Amersham Pharmacia Biotech) and eluted with 10 mM reduced glutathione. GST-DNA-PK, GST-Nek2, GST-Nop10 and active Cyclin-Cdk kinase complexes (Cyclin D1/Cdk4, Cyclin B/Cdc2, Cyclin E/Cdk2 and Cyclin A/Cdk2) were obtained from MBL Co. Ltd (Japan). Rb C-terminus (amino acids 701-928) was purchased from New England Biolabs (Beverly, MA, USA).

Antibodies

The generation and specificity of the 3D10 anti-human Lats2 monoclonal antibody has been previously described (Yabuta *et al.* 2000). To generate an anti-Aurora-A polyclonal antibody, rabbits were injected with a recombinant GST-fused full-length Aurora-A protein. The antisera were then affinity-purified against the protein. Anti-γ-tubulin polyclonal antibody (Sigma, St Louis, MO, USA) was purchased. Anti-HA polyclonal, anti-Cyclin B, anti-Myc and anti-GST monoclonal antibodies were obtained from MBL Co. Ltd.

Generation of anti-phospho-Ser83 monoclonal antibody and Western blotting

To establish a mouse hybridoma that produces anti-phospho-S83-Lats2 antibodies, mice were immunized subcutaneously with the KLH-conjugated phosphopeptide CREIRYS(PO_3H_2)LLPF (amino acids 78–87) emulsified in Freund's complete adjuvant. Thereafter, the mice were boosted four times at biweekly intervals with the KLH conjugate in Freund's incomplete adjuvant. B-cell hybridomas were generated from the spleen cells of these mice and the 3B11 anti-phospho-S83 antibody was affinity-purified by the phospho-antigen-peptide column. To eliminate non-specific antibodies reacting with the unphosphorylated antigen peptide, the antibody preparation was passed through a non-phospho-Lats2-peptide (CREIRYSLLPF) column. The specificity of the 3B11 antibody was confirmed by both Western blotting (shown in Fig. 3C) and ELISA (data not shown). To detect the *in vivo* phosphorylation of S83, immunoprecipitations were performed with 5 μg of either the 3D10 or 3B11 antibody, after which the immunoprecipitates were resolved by SDS–PAGE and transferred to polyvinylidene difluoride (PVDF) membranes (Millipore Corporation, Bedford, MA, USA). Western blotting was performed with 5 μg of 3D10 antibody in TBST (100 mM Tris-Cl, pH 7.5, 150 mM NaCl, 0.05% Tween-20) containing 1% BSA. Western blotting using antibodies other than 3D10 and 3B11 was performed in TBST containing 5% non-fat milk.

In vitro kinase assays and immunoprecipitations

In vitro kinase assays were performed with 1 μg of GST-purified kinases and 2 μg of GST-purified substrates for 30 min at 30 °C in kinase buffer (20 mM Tris-HCl, pH 7.5, 10 mM $MgCl_2$, 5 mM $MnCl_2$, 1 mM DTT, 1 mM NaF, 0.1 mM Na_3VO_4, 10 mM β-glycerophosphate) containing 20 μM ATP and 10 μCi [γ-^{32}P]ATP. To examine the interaction between 6Myc-Lats2 and 1-393 and GFP-Aurora-A, the transfected 293T cells were lysed in lysis buffer A (50 mM Tris-HCl, pH 7.5, 250 mM NaCl, 1 mM EDTA, 0.2% NP-40, 1 mM PMSF, 1 μg/mL aprotinin, 2 μg/mL leupeptin, 1 μg/mL pepstatine A, 1 mM NaF, 1 mM Na_3VO_4). After centrifugation, the clear lysates were immunoprecipitated with 2 μg of anti-Myc or anti-GFP antibodies for 3 h at 4 °C. The immune complexes were collected by adding 30 μL of 50% protein G sepharose (Amersham Pharmacia Biotech) slurry. The complexes were washed five times with lysis buffer B (50 mM Tris-HCl, pH 7.5, 50 mM NaCl, 1 mM EDTA, 0.1% NP-40).

Immunofluorescence staining

HeLa S3 cells that transiently expressed GFP-full length Lats2 or GFP alone were fixed by sequential incubations with 4% formaldehyde in PBS, 0.1% Triton X-100 in PBS and then 0.05% Tween-20 in PBS, each for 10 min at room temperature. To prepare mitotic cells, the transfected cells were blocked at the S phase by the addition of 2.5 mM thymidine for 22 h. They were then released from the block by replacing the medium with fresh medium without drugs. They were fixed 12 h later. After being washed, cells were incubated with anti-Aurora-A antibody or anti-γ-tubulin antibody, followed by incubation with Texas Red (Amersham Pharmacia Biotech) or AlexaFluor 594 (Molecular Probes, Eugene, OR, USA)-conjugated anti-rabbit/mouse immunoglobulin G as previously described (Tsuruga *et al.* 1997). To visualize 6Myc-Lats2 or its derivatives, cells expressing each 6Myc-Lats2 derivative were fixed and stained with anti-Myc antibody followed by Alexa-Fluor 488-conjugated anti-mouse immunoglobulin G. DNA was stained by Hoechst 33258 (Sigma). Immunofluorescence staining with the 3B11 antibody was performed as similar way. The stained cells were observed with an Axiophot microscope (Zeiss) or BX51 microscope (Olympus).

Acknowledgements

We thank Dr P. Hughes for critically reading the manuscript. This work was supported by a Grant-in-aid for Scientific Research on Priority Areas from the Ministry of Education, Culture, Sports, Science and Technology of Japan, and grants from the Osaka Cancer Society, the Yasuda Medical Research Foundation, the Welfide Medical Research Foundation, the Japanese Foundation for Multidisciplinary Treatment of Cancer and the Osaka Cancer Research Foundation.

References

Adams, R.R., Carmena, M. & Earnshaw, W.C. (2001) Chromosomal passengers and the (aurora) ABCs of mitosis. *Trends Cell Biol.* **11**, 49–54.

Anand, S., Penrthyn-Lowe, S. & Venkitaraman, A.R. (2003) AURORA-A amplification overrides the mitotic spindle assembly checkpoint, inducing resistance to Taxol. *Cancer Cell* **3**, 51–62.

Bischoff, J.R. & Plowman, G.D. (1999) The Aurora/Ipl1p kinase family: regulators of chromosome segregation and cytokinesis. *Trends Cell Biol.* **9**, 454–459.

Bischoff, J.R., Anderson, L., Zhu, Y., *et al.* (1998) A homologue of *Drosophila aurora* kinase is oncogenic and amplified in human colorectal cancers. The Aurora/Ipl1p kinase family: regulators of chromosome segregation and cytokinesis. *EMBO J.* **17**, 3052–3065.

Blagden, S.P. & Glover, D.M. (2003) Polar expeditions-provisioning the centrosome for mitosis. *Nature Cell Biol.* **5**, 505–511.

Chen, S.-S., Chang, P.-C., Cheng, Y.-W., Tang, F.-M. & Lin, Y.-S. (2002) Suppression of the STK15 oncogenic activity requires a transactivation-independent p53 function. *EMBO J.* **21**, 4491–4499.

Crosio, C., Fimia, M.F., Loury, R., *et al.* (2002) Mitotic phosphorylation of histone H3: spatio-temporal regulation by mammalian Aurora kinases. *Mol. Cell. Biol.* **22**, 874–885.

Doxsey, S. (2001) Re-evaluating centrosome function. *Nature Rev. Mol. Cell Biol.* **2**, 688–698.

Dutertre, S., Descamps, S. & Prigent, C. (2002) On the role of aurora-A in centrosome function. *Oncogene* **21**, 6175–6183.

Eyers, P.A., Erikson, E., Chen, L.G. & Maller, J.L. (2003) A novel mechanism for activation of the protein kinase Aurora A. *Curr. Biol.* **13**, 691–697.

Farruggio, D.C., Townsley, F.M. & Ruderman, J.V. (1999) Cdc20 associates with the kinase aurora2/Aik. *Proc. Natl. Acad. Sci. USA* **96**, 7306–7311.

Fry, A.M., Schultz, S.J., Bartek, J. & Nigg, E.A. (1995) Substrate specificity and cell cycle regulation of the Nek2 protein kinase, a potential human homolog of the mitotic regulator NIMA of *Aspergillus nidulans*. *J. Biol. Chem.* **270**, 12899–12905.

Giet, R. & Prigent, C. (1999) Aurora/Ipl1p-related kinases, a new oncogenic family of mitotic serine-threonine kinases. *J. Cell Sci.* **112**, 3591–3601.

Giet, R., McLean, D., Descamps, S., *et al.* (2002) *Drosophila* Aurora A kinase is required to localize D-TACC to centrosomes and to regulate astral microtubules. *J. Cell Biol.* **156**, 437–451.

Glover, D.M., Leibowitz, M.H., McLean, D.A. & Parry, H. (1995) Mutations in aurora prevent centrosome separation leading to the formation of monopolar spindles. *Cell* **81**, 95–105.

Henras, A., Henry, Y., Bousquet-Antonelli, C., *et al.* (1998) Nhp2p and Nop10p are essential for the function of H/ACA snoRNPs. *EMBO J.* **17**, 7078–7090.

Hirota, T., Morisaki, T., Nishiyama, Y., *et al.* (2000) Zyxin, a regulator of actin filament assembly, targets the mitotic apparatus by interacting with h-warts/LATS1 tumor suppressor. *J. Cell Biol.* **149**, 1073–1086.

Hirota, T., Kunitoku, N., Sasayama, T., *et al.* (2003) Aurora-A and an interacting activator, the LIM protein Ajuba, are required for mitotic commitment in human cells. *Cell* **114**, 585–598.

Hori, T., Takahori-Kondo, A., Kamikubo, Y. & Uchiyama, T. (2000) Molecular cloning of a novel human protein kinase, kpm, that is homologous to warts/lats, a *Drosophila* tumor suppressor. *Oncogene* **19**, 3101–3109.

Justice, R.W., Zelian, O., Woods, D.F., Noll, M. & Bryant, P.J. (1995) The *Drosophila* tumor suppressor gene *warts* encodes a homolog of human myotonic dystrophy kinase and is required for the control of cell shape and proliferation. *Genes Dev.* **9**, 534–546.

Kamikubo, Y., Takaori-Kondo, A., Uchiyama, T. & Hori, T. (2003) Inhibition of cell growth by conditional expression of kpm, a human homologue of *Drosophila* warts/lats tumor suppressor. *J. Biol. Chem.* **278**, 17609–17614.

Katayama, H., Zhou, H., Li, Q., Tatsuka, M. & Sen, S. (2001) Interaction and feedback regulation between STK15/BTAK/Aurora-A kinase and protein phosphatase 1 through mitotic cell division cycle. *J. Biol. Chem.* **276**, 46219–46224.

Kim, S.-T., Lim, D.-S., Canman, C.E. & Kastan, M. (1999) Substrate specificities and identification of putative substrates of ATM kinase family members. *J. Biol. Chem.* **274**, 37538–37543.

Kimura, M., Matsuda, Y., Yoshioka, T. & Okano, Y. (1999) Cell cycle-dependent expression and centrosome localization of a third human aurora/Ipl1-related protein kinase, AIK3. *J. Biol. Chem.* **274**, 7334–7340.

Kitagawa, M., Higashi, H., Jung, H.K., *et al.* (1996) The consensus motif for phosphorylation by cyclin D1-Cdk4 is different from that for phosphorylation by cyclin A/E-Cdk2. *EMBO J.* **15**, 7060–7069.

Kufer, T.A., Sillje, H.H., Korner, R., *et al.* (2002) Human TPX2 is required for targeting Aurora-A kinase to the spindle. *J. Cell Biol.* **158**, 617–623.

Li, Y., Pei, J., Xia, H., *et al.* (2003) Lats2, a putative tumor suppressor, inhibits G1/S transition. *Oncogene* **22**, 4398–4405.

Mayor, T., Meraldi, P., Stierhof, Y.D., Nigg, E.A. & Fry, A.M. (1999) Protein kinases in control of the centrosome cycle. *FEBS Lett.* **452**, 92–95.

Meraldi, P., Honda, R. & Nigg, E.A. (2002) Aurora-A overexpression reveals tetraploidization as a major route to centrosome amplification in p53-/- cells. *EMBO J.* **21**, 483–492.

Morisaki, T., Hirota, T., Iida, S., *et al.* (2002) WARTS tumor suppressor is phosphorylated by Cdc2/cyclin B at spindle poles during mitosis. *FEBS Lett.* **529**, 319–324.

Nigg, E.A. (2001) Mitotic kinases as regulators of cell division and its checkpoints. *Nature Rev. Mol. Cell Biol.* **2**, 21–32.

Nigg, E.A. (2002) Centrosome aberrations: cause or consequence of cancer progression? *Nature Rev. Cancer* **2**, 815–825.

Nishiyama, Y., Hirota, T., Morisaki, T., *et al.* (1999) A human homolog of *Drosophila warts* tumor suppressor, h-warts, localized to mitotic apparatus and specifically phosphorylated during mitosis. *FEBS Lett.* **459**, 159–165.

Shindo, M., Nakano, H., Kuroyanagi, H., *et al.* (1998) cDNA cloning, expression, subcellular localization, and chromosomal assignment of mammalian aurora homologues, aurora-related kinase (ARK) 1 and 2. *Biochem. Biophys. Res. Commun.* **244**, 285–292.

Smits, V.A., Klompmaker, R., Arnaud, L., *et al.* (2000) Polo-like kinase-1 is a target of the DNA damage checkpoint. *Nature Cell Biol.* **2**, 672–676.

St. John, M.A.R., Tao, W., Fei, X., *et al.* (1999) Mice deficient of *Lats1* develop soft-tissue sarcomas, ovarian tumours and pituitary dysfunction. *Nature Genet.* **21**, 182–186.

Tao, W., Zhang, S., Turenchalk, G.S., *et al.* (1999) Human homologue of the *Drosophila melanogaster lats* tumour suppressor modulates CDC2 activity. *Nature Genet.* **21**, 177–181.

Tatsuka, M., Katayama, H., Ota, T., *et al.* (1998) Multinuclearity and increased ploidy caused by overexpression of the aurora- and Ipl1-like midbody-associated protein mitotic kinase in human cancer cells. *Cancer Res.* **58**, 4811–4816.

Tsai, M.Y., Wiese, C., Cao, K., *et al.* (2003) A Ran signalling pathway mediated by the mitotic kinase Aurora A in spindle assembly. *Nature Cell Biol.* **5**, 242–248.

Tseng, T.C., Chen, S.H., Hsu, Y.P. & Tang, T.K. (1998) Protein kinase profile of sperm and eggs: cloning and characterization of two novel testis-specific protein kinases (AIE1, AIE2) related to yeast and fly chromosome segregation regulators. *DNA Cell Biol.* **17**, 823–833.

Tsuruga, H., Yabuta, N., Hosoya, S., *et al.* (1997) *HsMCM6*: a new member of the human MCM/P1 family encodes a protein homologous to fission yeast Mis5. *Genes Cells* **2**, 381–399.

Xia, H., Qi, H., Li, Y., *et al.* (2002) LATS1 tumor suppressor regulates G2/M transition and apoptosis. *Oncogene* **21**, 1233–1241.

Xu, T., Wang, W., Zhang, S., Stewart, R.A. & Yu, W. (1995) Identifying tumor suppressors in genetic mosaics: the *Drosophila lats* gene encodes a putative protein kinase. *Development* **121**, 1053–1063.

Yabuta, N., Fujii, T., Copeland, N.G., *et al.* (2000) Structure, expression, and chromosome mapping of *LATS2*, a mammalian homologue of the *Drosophila* tumor suppressor gene *lats/warts*. *Genomics* **63**, 263–270.

Yang, X., Li, D.M., Chen, W. & Xu, T. (2001) Human homologue of *Drosophila lats*, LATS1, negatively regulate growth by inducing G(2)/M arrest or apoptosis. *Oncogene* **20**, 6516–6523.

Zhou, H., Kuang, J., Zhong, L., *et al.* (1998) Tumour amplified kinase STK15/BTAK induces centrosome amplification, aneuploidy and transformation. *Nature Genet.* **20**, 189–193.

Received: 14 October 2003
Accepted: 2 February 2004

Mcp6, a meiosis-specific coiled-coil protein of *Schizosaccharomyces pombe*, localizes to the spindle pole body and is required for horsetail movement and recombination

Takamune T. Saito, Takahiro Tougan, Daisuke Okuzaki, Takashi Kasama and Hiroshi Nojima*

Department of Molecular Genetics, Research Institute for Microbial Diseases, Osaka University, 3-1 Yamadaoka, Suita, Osaka 565-0871, Japan
*Author for correspondence (e-mail: snj-0212@biken.osaka-u.ac.jp)

Accepted 3 November 2004
Journal of Cell Science 118, 447-459 Published by The Company of Biologists 2005
doi:10.1242/jcs.01629

Summary

We report here that a meiosis-specific gene of *Schizosaccharomyces pombe* denoted *mcp6*$^+$ (meiotic coiled-coil protein) encodes a protein that is required for the horsetail movement of chromosomes at meiosis I. The *mcp6*$^+$ gene is specifically transcribed during the horsetail phase. Green fluorescent protein (GFP)-tagged Mcp6 appears at the start of karyogamy, localizes to the spindle-pole body (SPB) and then disappears before chromosome segregation at meiosis I. In the *mcp6Δ* strain, the horsetail movement was either hampered (zygotic meiosis) or abolished (azygotic meiosis) and the pairing of homologous chromosomes was impaired. Accordingly, the allelic recombination rates of the *mcp6Δ* strain were only 10-40% of the wild-type rates. By contrast, the ectopic recombination rate of the *mcp6Δ* strain was twice the wild-type rate. This is probably caused by abnormal homologous pairing in *mcp6Δ* cells because of aberrant horsetail movement. Fluorescent microscopy indicates that SPB components such as Sad1, Kms1 and Spo15 localize normally in *mcp6Δ* cells. Because Taz1 and Swi6 also localized with Sad1 in *mcp6Δ* cells, Mcp6 is not required for telomere clustering. In a *taz1Δ* strain, which does not display telomere clustering, and the *dhc1-d3* mutant, which lacks horsetail movement, Mcp6 localized with Sad1 normally. However, we observed abnormal astral microtubule organization in *mcp6Δ* cells. From these results, we conclude that Mcp6 is necessary for neither SPB organization nor telomere clustering, but is required for proper astral microtubule positioning to maintain horsetail movement.

Supplementary material available online at
http://jcs.biologists.org/cgi/content/full/118/2/447/DC1

Key words: Meiosis, *S. pombe*, SPB, Recombination, Pairing, Horsetail

Introduction

Sexually reproducing eukaryotic organisms undergo meiosis, a special type of cell division, to generate inheritable haploid gametes from diploid parental cells. This process includes meiosis-specific events that increase genetic diversity, such as synaptonemal complex (SC) formation, homologous pairing and recombination. The fission yeast *Schizosaccharomyces pombe* proceeds to meiosis when it is nutritionally starved. At this point, two cells with opposite mating types conjugate and the two haploid nuclei fuse, thereby producing a zygote with a diploid nucleus; the meiotic process immediately follows this. Efficient pairing of the homologous chromosomes and the subsequent processing and completion of recombination during the meiotic prophase are pivotal for achieving correct chromosome segregation during meiotic division. An essential event for efficient chromosome pairing in *S. pombe* is the clustering during prophase of meiosis I of the telomeres of three chromosomes near the spindle-pole body (SPB) (Chikashige et al., 1994; Chikashige et al., 1997). This characteristic arrangement of meiotic chromosomes has been observed in a wide range of organisms and is denoted a 'bouquet' arrangement (Loidl, 1990; Scherthan, 2001; Zickler and Kleckner, 1999). This arrangement has been proposed to facilitate homologous chromosome pairing because it generates a polarized chromosome configuration by bundling chromosomes together at their telomeres.

The clustering of telomeres occurs during an event termed horsetail nuclear movement that is characteristic of *S. pombe*. It occurs at prophase I of meiosis and is characterized by a dynamic oscillation of the nucleus and the adoption by the nucleus of an elongated morphology (Chikashige et al., 1994). This movement has been proposed to facilitate the pairing of homologous chromosomes because it causes the chromosomes, which are aligned in the same direction as a result of bundling at their telomeric ends, to be shuffled around each other (Chikashige et al., 1994; Kohli, 1994; Hiraoka, 1998; Yamamoto et al., 1999; Yamamoto and Hiraoka, 2001). Thus, it enhances the chance that a chromosome encounters its correct partner and thereby promotes the linkage of homologous pairs of chromosomes through homologous recombination. In support of this notion, homologous recombination is reduced in mutants that display impaired

telomere clustering owing to the depletion of protein components of the telomere or the SPB, even though recombination machinery is intact in these mutants. For example, elimination of the telomere-binding protein Taz1 (Cooper et al., 1998; Nimmo et al., 1998) or Rap1 (Kanoh and Ishikaw, 2001), or depletion of the SPB component Kms1 (Shimanuki et al., 1997; Niwa et al., 2000) results in a loss of telomere-SPB clustering and reduced meiotic recombination.

It has been proposed that horsetail nuclear movement is predominantly established by pulling the astral microtubules that link the SPB to microtubule-anchoring sites, and that the pulling force is provided by cytoplasmic dynein (Chikashige et al., 1994; Svoboda et al., 1995; Ding et al., 1998; Yamamoto and Hiraoka, 2003). Thus, homologous recombination is also reduced when nuclear oscillation is abolished by disrupting the *dhc1*$^+$ gene, which encodes dynein heavy chain (DHC), a major component of cytoplasmic dynein that is localized to microtubules and the SPB (Yamamoto et al., 1999). It was proposed that dynein drives this nuclear oscillation by mediating the cortical microtubule interactions and regulating the dynamics of microtubule disassembly at the cortex (Yamamoto et al., 2001). Meiotic recombination is also reduced in a null mutant of the *dlc1*$^+$ gene that encodes an SPB protein that belongs to the dynein-light-chain family (Miki et al., 2003). In this mutant, Dhc1-dependent nuclear movement during meiotic prophase is irregular in its duration and direction. This model explains some of the regulatory mechanisms behind nuclear oscillation and chromosome pairing. However, the details of these mechanisms are still mostly unknown. The identification of additional regulatory components is needed fully to elucidate these processes.

In the course of our functional characterization of meiotic-specific proteins that harbour coiled-coil motifs, we found a new SPB-associated protein that is required for meiotic nuclear oscillation and recombination. This gene is expressed specifically during meiosis and thus is referred to as *mcp6*$^+$ (meiotic coiled-coil protein). The coiled-coil motif, which consists of two to five amphipathic α-helices that twist around one another to form a supercoil, is known to be required for protein-protein interaction (Burkhard et al., 2001). In the present study, we report our functional analysis of this protein.

Materials and Methods

Yeast strains, media and molecular biology

The *S. pombe* strains used in this study are listed in Table 1. Complete media YPD or YE, the synthetic minimal medium EMM2 and the sporulation media ME or EMM2-N (1% glucose) were used (Alfa et al., 1993). Homozygous diploid strains were constructed by cell fusion. Cells were converted to protoplasts by treatment with lysing enzyme. Then, cells were fused using $CaCl_2$ and polyethylene glycol (Sipiczki and Ferenczy, 1977). Plates with EMM2 containing 1 M sorbitol were used in the cell fusion experiments. Induction of meiosis in the genetic background of the *pat1-114* mutant (Shimada et al., 2002). Northern (Watanabe et al., 2001) and western blot (Okuzaki et al., 2003) analyses were performed as described previously.

Gene disruption

To disrupt the *mcp6*$^+$ gene by replacing it with the *ura4*$^+$ gene, we used the polymerase chain reaction (PCR) to obtain a DNA fragment carrying the 5′ upstream region and 3′ downstream region of the *mcp6*$^+$ gene. For this purpose, we synthesized the following four oligonucleotides and used them as primers: mcp6-5F, 5′-GGTACCTTCTGGTGCCGCCGACCTTC-3′; mcp6-5R, 5′-CTCGAGATTAAATCAATCTGTTAATC-3′; mcp6-3F, 5′-CCCGGGGGATAGCTATGAAACCCTGA-3′; mcp6-3R, 5′-GAGCTCTCATTTTTTTTATAAGAAGG-3′. (The underlined sequences denote the artificially introduced restriction enzyme sites for *Kpn*I, *Xho*I, *Sma*I and *Sac*I, respectively.) These PCR products and the 1.8 kb *Hin*dIII fragment containing the *ura4*$^+$ gene (Grimm et al., 1988) were inserted into the pBluescriptII KS (+) vector via the *Kpn*I-*Xho*I, *Sma*I-*Sac*I or *Hin*dIII sites. This plasmid construct was digested with *Kpn*I and *Sac*I, and the resulting construct was introduced into the diploid strain TP4-5A/TP4-1D. The Ura$^+$ transformants were then screened by Southern blot analysis to identify the disrupted strain.

Construction of strains harbouring integrated *mcp6*$^+$-tag genes

To construct green fluorescent protein (GFP)-tagged *mcp6*$^+$ strains, we performed PCR using the wild-type (TP4-5A) genome as a template and obtained a DNA fragment carrying the open reading frame (ORF) region and the 3′ downstream region of the *mcp6*$^+$ gene. For this purpose, we synthesized the following two oligonucleotides and used them as primers: mcp6-ORF-F, 5′-CGGCGCGCCGCATATGGAATATCAAGAAGAGGC-3′; mcp6-ORF-R, 5′-GTACTCGAGGCGGCCGCGGGCTCAGATCGTGATTGACAG3′. The underlined sequences denote the artificially introduced restriction enzyme sites for *Asc*I and *Nde*I, and *Xho*I and *Not*I, respectively. To obtain the 3′ downstream region, we used the same primers as described above. These PCR products were inserted into the pTT(GFP)-Lys3 vector (T.T., unpublished) (see supplementary material Fig. S1), which is designed to allow one-step integration via *Nde*I-*Not*I and *Sma*I-*Sac*I sites. This plasmid construct was digested with *Pme*I. The resulting construct was introduced into strain HM105 (*h*$^-$ *lys3*). We then screened the Lys$^+$ transformants and confirmed the precise integration of the constructs by PCR.

Recombination frequency and spore viability

The crossing-over rate was determined as described previously (Fukushima et al., 2000). Briefly, haploid parental strains were grown on YPD plates at 30°C and cells were mated and sporulated on ME plates at 28°C (zygotic meiosis). After 1 day of incubation, the spores were separated by a micromanipulator (Singer Instruments, UK). To examine the frequency of crossing over, we measured the genetic distance (in centiMorgans) between *leu1*$^+$ and *his2*$^+$, and between *lys3*$^+$ and *cdc12*$^+$. Genetic distance was calculated according to the formula $50\times[T+(6\times NPD)]+(PD+T+NPD)$ (Perkins, 1949), where *T*, *NPD* and *PD* indicate the number of tetratypes, nonparental ditypes and parental ditypes, respectively.

Intragenic recombination rate and spore viability were determined as described previously (Shimada et al., 2002). Briefly, haploid parental strains were grown on YPD plates at 33°C. Cells were mated and sporulated on ME plates at 28°C (zygotic meiosis). After 3-4 days of incubation, spores were treated with 1% glusulase (NEN Life Science Products) for 2-3 hours at room temperature and checked under a microscope for complete digestion of contaminating vegetative cells. The glusulase-treated spores were then washed with water and used to measure the intragenic recombination rate and in the spore-viability assays. To examine the frequency of intragenic or ectopic recombination (or prototroph frequency), we used two *ade6* alleles – *ade6-M26* and *ade6-469* (Gutz, 1971) or *ade6-M26* and z7 (*ade6-469*) (Virgin and Bailey, 1998), because the reciprocal recombination between these alleles produces the *ade6*$^+$ allele.

Fluorescent microscopic observations

Cells from a single colony were cultured at 28°C in 10 ml EMM2 plus supplements [adenine (75 μg/ml), histidine (75 μ/ml), leucine (250

Table 1. Strains used in this study

Strain	Genotype	Source†
CD16-1	*h⁺/h⁻ ade6-M210/ade6-M216 cyh1/⁺ ⁺/lys5-391*	C. Shimoda (Osaka City University, Osaka, Japan)
CD16-5	*h⁻/h⁻ ade6-M210/ade6-M216 cyh1/⁺ ⁺/lys5-391*	C. Shimoda
ST194	*h⁻/h⁻ ade6-M216/210 leu1-32/leu1-32 mcp6::[mcp6-GFP-3'UTR-Lys3⁺]/mcp6::[mcp6-GFP-3'UTR-Lys3⁺] pat1-114/pat1-114*	
ST142	*h⁹⁰ ade6-M216 leu1-32 ura4-D18 mcp6::[mcp6-GFP-3'UTR-Lys3⁺] dsRed-Sad1 [::LEU2]*	
JZ670	*h⁻/h⁻ ade6-M210/ade6-M216 leu1-32/leu1-32 pat1-114/pat1-114*	M. Yamamoto (University of Tokyo, Tokyo, Japan)
TT405	*h⁻/h⁻ ade6-M216/210 leu1-32/leu1-32 ura4-D18/ura4-D18 mcp6::ura4⁺/mcp6::ura4⁺ pat1-114/pat1-114*	
CT026-1*	*h⁹⁰ leu1-32 ura4-D18 TB19::GFP-lys1⁺*	Y. Hiraoka (Kansai Advanced Research Center, Kobe, Japan)
ST193*	*h⁹⁰ leu1-32 ura4-D18 mcp6::ura4⁺ TB19::GFP-lys1⁺*	
AY174-7B	*h⁹⁰ leu1-32 ura4-D18 ade6-M210 his7::lacI-GFP-NLS-his7⁺ lys1::lacOr-lys1⁺*	K. Nabeshima (Stanford University, Stanford, CA) and A. Yamamoto (Kansai Advanced Research Center, Kobe, Japan)
ST197	*h⁹⁰ leu1-32 ura4-D18 mcp6::ura4⁺ his7::lacI-GFP-NLS-his7⁺ lys1::lacOr-lys1⁺*	
TT8-1	*h⁻ ura4⁺*	
NP32-2A	*h⁺ leu1-32 his2 ura4-D18*	Nabeshiwa et al., 2001
TT232-1	*h⁺ his2 leu1-32 ura4-D18 lys3 cdc12*	
MS105-1B	*h⁻ ade6-M26 ura4-D18*	Shimada et al., 2002
MS111w1	*h⁺ ade6-469 ura4-D18 leu1-32 his2*	Shimada et al., 2002
GP1123	*h⁺ ade6-D1 ura4-D18 leu1-32 zzz7::[ade6-469 ura4⁺]*	G. Smith
TT398	*h⁻ ura4-D18 mcp6::ura4⁺*	
TT399	*h⁺ his2 leu1-32 ura4-D18 mcp6::ura4⁺*	
TT411	*h⁻ ura4-D18 mcp6::ura4⁺ cdc12 lys3*	
TT400	*h⁻ ade6-M26 ura4-D18 mcp6::ura4⁺*	
TT401	*h⁺ ade6-469 his2 leu1-32 ura4-D18 mcp6::ura4⁺*	
TT1014	*h⁺ ade6-D1 leu1-32 ura4-D18 mcp6::ura4⁺ zzz7::[ade6-469 ura4⁺]*	
TP4-5A	*h⁻ ade6-M210 ura4-D18 leu1-32*	C. Shimoda
TP4-1D	*h⁺ ade6-M216 his2 leu1-32 ura4-D18*	C. Shimoda
TT397-5A	*h⁻ ade6-M210 leu1-32 ura4-D18 mcp6::ura4⁺*	
TT397-1D	*h⁺ ade6-M216 his2 leu1-32 ura4-D18 mcp6::ura4⁺*	
CRL790	*h⁹⁰ ade6-216 leu1-32 ura4-D18 lys1 dsRed-Sad1 [::LEU2]*	Y. Hiraoka
ST148	*h⁹⁰ ade6-M216 leu1-32 ura4-D18 mcp6::ura4⁺ dsRed-Sad1[::LEU2]*	
ST176	*h⁹⁰ leu1-32 ura4-D18(or⁺) dsRed-sad1[::LEU2] spo15-GFP::LEU2*	
ST171-1	*h⁹⁰ ade6-M210 leu1-32 ura4-D18(or⁺) mcp6::ura4⁺ dsRed-sad1[::LEU2] spo15-GFP::LEU2*	
ST191-1	*h⁹⁰ leu1-32(or⁺) dsRed-sad1[::LEU2] kms1::GFP::Kanr*	
ST172-1	*h⁹⁰ ura4-D18(or⁺) mcp6::ura4+ dsRed-sad1[::LEU2] kms1::GFP::Kanr*	
ST178	*h⁹⁰ ade6-M216 leu1-32(or⁺) ura4-D18(or⁺) dsRed-sad1[::LEU2] Taz1::GFP::Kanr*	
ST173	*h⁹⁰ ade6-M216 ura4-D18(or⁺) mcp6::ura4⁺ dsRed-sad1[::LEU2] Taz1::GFP::Kanr*	
ST179-1	*h⁹⁰ leu1-32 ura4-D18 dsRed-sad1[::LEU2] swi6⁺::GFP:leu2*	
ST174	*h⁹⁰ leu1-32 ura4-D18 mcp6::ura4⁺ dsRed-sad1[::LEU2] swi6⁺::GFP:leu2*	
YY105	*h⁹⁰ leu1-32 ura4-D18 lys1::nmt1pGFP-alpha2tubulin*	Y. Hiraoka
ST146	*h⁹⁰ leu1-32 ura4-D18 mcp6::ura4⁺ lys1::nmt1pGFP-alpha2tubulin*	
ST134	*h⁹⁰ ade6-M210 leu1-32 ura4-D18 mcp6::[mcp6-GFP-3'UTR-Lys3⁺]*	
ST196-1	*h⁹⁰ ade6-M210 leu1-32 dhc1-d3[LEU2] mcp6::[mcp6-GFP-3'UTR-Lys3⁺] dsRed-Sad1[::LEU2]*	
ST200	*h⁹⁰ ade6-M210 leu1-32 ura4-D18 taz1::ura4⁺ mcp6::[mcp6-GFP-3'UTR-Lys3⁺]*	

*TB19 signifies the N-terminal portion of DNA polymerase α (Ding et al., 2000).
†Unattributed strains were constructed for this study.

μg/ml), lysine (75 μg/ml) and uracil (75 μ/ml)] until they reached mid-log phase. The cells were collected by centrifugation, washed three times with 1 ml EMM2-N and then induced to enter meiosis by incubation in EMM2-N at 28°C for 6 hours. For live observations, we added 0.5 μg ml^{-1} Hoechst 33342 to 200 μl of the cells and an aliquot was observed under a fluorescence microscope (Olympus BX51).

For methanol fixation, cells were collected by aspiration through a glass filter (particle retention 1.2 μm; Whatman, Brentford, UK) that traps cells. The cells were then immediately immersed into methanol at −80°C and left overnight to fix the cells. The cells were then washed off the glass filter with distilled water and collected by centrifugation (2000 *g*, 5 minutes), and the pellet was washed three times with PBS. 0.5 μg ml^{-1} Hoechst 33342 was added and the cells were observed under a fluorescence microscope.

For time-lapse observations, cells expressing GFP-tagged DNA polymerase α (Polα) (ST193 and CRL026-1) or cells expressing LacI-NLS-GFP and integrated LacO repeat at *lys1* locus (ST197 and AY174-7B) were cultured in 10 ml EMM2 plus supplements until they reached mid-log phase at 28°C. They were then induced to enter meiosis by incubation in EMM2-N at 28°C. After 5 hours of nitrogen starvation, the cells were put on a glass-bottomed dish whose surface was coated with 0.2% concanavalin A and images under a fluorescence microscope (Olympus IX71) were recorded every 2.5 minutes (1 second of exposure time) after the initiation of karyogamy. For observation of LacI-GFP dots, images were taken with a 0.3 second exposure at 5 minute intervals, with ten optical sections made at 0.5 μm intervals for each time point. Projected images obtained with Meta Morph software were analysed.

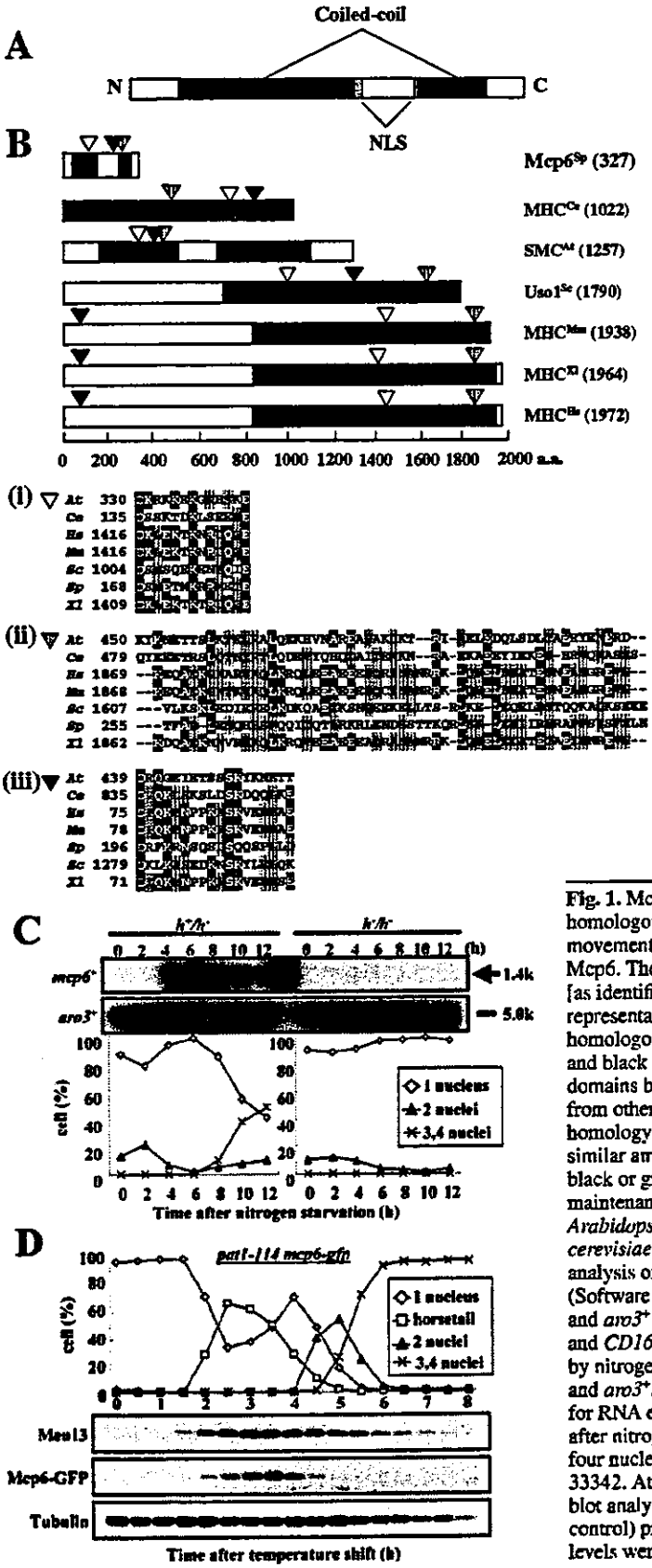

Immunofluorescence

Cells were fixed following the procedure of Hagan and Hyams (Hagan and Hyams, 1988) using glutaraldehyde and paraformaldehyde. In indirect immunofluorescence microscopy (Hagan and Yanagida, 1995), the SPB was stained with the anti-Sad1 antibody (a gift from O. Niwa, Kazusa DNA Research Institute, Kisatazu, Japan), microtubules were stained with the anti-α-tubulin antibody (TAT1). Subsequently, we added an Alexa-488-conjugated goat anti-mouse antibody (Molecular Probes, Eugene, OR) to label TAT1 or an Alexa-594-conjugated goat anti-rabbit antibody (Molecular Probes, Eugene, OR) to label anti-Sad1 antibody. The samples were then stained with 0.2 mg ml^{-1} Hoechst 33342 in PBS for 1 minute and mounted with antifade mounting medium containing 10 mg/ml *p*-phenylendiamine in 100 mM Tris-HCl (pH 8.8). Fluorescence images of these cells were observed using a fluorescence microscope (Olympus BX51) with a Cool SNAP CCD camera (Roper Scientific, San Diego, CA). Immunofluorescence images were acquired using Adobe Photoshop 7.0.

Results

Mcp6 is an *S.-pombe*-specific coiled-coil protein

Meu13 harbours a coiled-coil motif and plays a pivotal role in homologous pairing, meiotic recombination at meiosis I (Nabeshima et al., 2001) and the meiotic recombination checkpoint (Shimada et al., 2002). To identify a meiosis-specific coiled-coil protein of *S. pombe* that might interact with Meu13, we searched the genome database for uncharacterized genes that harbour coiled-coil motifs (http://www.sanger.ac.uk/Projects/S_pombe/) and found 60 genes. We then obtained DNA fragments from each of these genes and used them as probes for time-course northern blot analysis to examine their meiosis-specific

Fig. 1. Mcp6 is a meiosis-specific coiled-coil protein that harbours three homologous regions conserved in other proteins that are involved in the movement of subcellular components. (A) Schematic representation of Mcp6. The locations of the two coiled-coil motifs and the NLSs are indicated [as identified by PSORT II (http://psort.nibb.ac.jp/)]. (B) Schematic representation of Mcp6-related proteins of other species. The locations of homologous domains in these proteins are denoted by vertical white, grey and black arrowheads. Multiple sequence alignment shows homologous domains between Mcp6 from *S. pombe* (denoted *Sp*) and the related proteins from other species. Gaps inserted in the alignment to attain maximal homology are indicated by hyphens. The amino acids that are identical or similar among four or more of the seven species examined are shaded in black or grey. Abbreviations: MHC, myosin heavy chain; SMC, structural maintenance of chromosomes; Sp, *Schizosaccharomyces pombe*; At, *Arabidopsis thaliana*; Ce, *Caenorhabditis elegans*; Sc, *Saccharomyces cerevisiae*; Mm, *Mus musculus*; Xl, *Xenopus laevis*; Hs, *Homo sapiens*. The analysis of DNA sequences was performed by using the GENETYX program (Software Development, Tokyo, Japan). (C) Northern blot analysis of *mcp6*$^+$ and *aro3*$^+$ (loading control). Total RNA was extracted from *CD16-1* (h^+/h^+) and *CD16-5* (h^-/h^-) cells at the indicated times after the induction of meiosis by nitrogen starvation. RNA was blotted and probed with the ORFs of *mcp6*$^+$ and *aro3*$^+$. The graph below indicates the meiotic profiles of the cells used for RNA extraction. The progression of meiosis was monitored every 2 hours after nitrogen starvation. The numbers of cells that bear one, two, three or four nuclei were assessed by counting the nuclei stained with Hoechst 33342. At least 200 cells were counted under the microscope. (D) Western blot analysis of the production of Mcp6-GFP and Meu13 (meiotic timing control) proteins during the synchronous meiosis of strain ST194. Tubulin levels were also examined as a loading control.